

Evolution of chemotaxis in stochastic environments

Martin Godány

A dissertation submitted in partial fulfillment
of the requirements for the degree of
Doctor of Philosophy
of
University College London.

Division of Infection & Immunity
University College London

September 3, 2015

I, Martin Godány, confirm that the work presented in this thesis is my own. Where information has been derived from other sources, I confirm that this has been indicated in the thesis. Specifically:

Chapter 2 This Chapter was derived from a submitted paper and includes contributions by Martin Godány, Bhavin S. Khatri and Richard A. Goldstein.

Abstract

Most of our understanding of bacterial chemotaxis comes from studies of *Escherichia coli*. However, recent evidence suggests significant departures from the *E. coli* paradigm in other bacterial species. In the first part of this work, we argue that the observed departures may stem from different species inhabiting distinct environments and thus adapting differently to specific environmental pressures. We therefore study the performance of various chemotactic strategies under a range of stochastic time- and space-varying attractant distributions *in silico*. We describe a novel type of response in which the bacterium tumbles more when attractant concentration is increasing, in contrast to the “adaptive” response of *E. coli*, and demonstrate how this response explains the behavior of aerobically-grown *Rhodobacter sphaeroides*. In this “speculator” response, bacteria compare the current attractant concentration to the long-term average. By tumbling persistently when the current concentration is higher than the average, bacteria maintain their position in regions of high attractant concentration. If the current concentration is lower than the average, or is declining, bacteria swim away in search of more favorable conditions. When the attractant distribution is spatially complex but slowly-changing, this response is as effective as that of *E. coli*. In the latter part of this work, we show that optimal response sensitivity is high for both adaptive and speculator responses. We argue that response sensitivity would increase over long evolutionary timescales and show that increases in response sensitivity could drive the evolution of adaptive and speculator responses.

Contents

1	Introduction	13
1.1	Chemotaxis in biological processes	14
1.2	Types of motility and taxis	15
1.2.1	Motility	15
1.2.2	Taxis	15
1.2.2.1	Energy taxis	15
1.3	Chemotaxis in <i>E. coli</i>	16
1.3.1	Behaviour	16
1.3.2	Biochemistry	17
1.3.3	Properties of the chemotactic response	18
1.4	Chemotaxis in other bacteria	19
1.4.1	Behaviour	19
1.4.2	Biochemistry	20
1.5	Evolution of chemotaxis	21
1.6	Aims	22
2	Optimal chemotactic responses in stochastic environments	23
2.1	Introduction	23
2.2	Methods	24
2.2.1	Simulation overview	24
2.2.2	Stochastic attractant distribution	24
2.2.3	Chemotaxis	26
2.2.4	Mutagenesis	29
2.2.5	Fitness	29
2.2.6	Selection	29
2.3	Results	30
2.3.1	Effects of environment on the chemotactic performance	30

2.3.2	Speculator response	31
2.3.3	Exploitation versus exploration in chemotaxis	33
2.3.4	Optimal response parameters and their dependence on T and L	35
2.3.4.1	Adaptive response	35
2.3.4.2	Inverted response	35
2.4	Discussion	39
3	Response sensitivity as a driver for the evolution of chemotaxis	43
3.1	Introduction	43
3.2	Methods	44
3.3	Results	45
3.3.1	Transitions between responses due to changing response sensitivity	45
3.3.2	Dependence of fitness and optimal response parameters on sensitivity	47
3.3.3	Perfect adaptation	51
3.4	Discussion	53
4	Conclusion	57
A	Dynamics of the attractant distribution	61
B	Dynamics of optimised adaptive, inverted and speculator responses	63
	Bibliography	63

List of Figures

2.1	Examples of the stochastic attractant distribution	25
2.2	Illustrative examples of the response function and corresponding timecourses of α in response to attractant step functions. Timecourses of α in response to attractant step functions for optimised responses.	28
2.3	Fitnesses of the optimised responses as a function of T and L	30
2.4	Curve-fit of our model of the speculator response to the digitised data of [1]	32
2.5	Exploration versus exploration in adaptive and speculator responses	34
2.6	Sensitivity as a function of T and L in the adaptive response	37
2.7	τ as a function of T and L in the inverted response	37
2.8	τ as a function of T and L in the adaptive response	38
2.9	β as a function of T and L in the inverted response	38
2.10	β as a function of T and L in the speculator response	39
3.1	Fitnesses and values of A , B and B/A as a function of evolutionary time in simulations with constrained maximum σ	46
3.2	$R(t)$ and $\alpha(t)$ for responses from generation 10000 of the 3 replicate simulations from Figure 3.1	48
3.3	Fitness of the delayed inverted response as a function of T and L	49
3.4	Fitness, scaled fitness, β , τ and B/A as a function of σ for different chemotactic strategies	50
3.5	Fitness and τ as a function of B/A in the adaptive response	52
3.6	Fitness as a function of B/A in adaptive response optimised under $B/A = -1$ for different combinations of T and L	54

List of Tables

2.1	Range of optimal response parameters at $T = 10^3, L = 50$	36
-----	--	----

Chapter 1

Introduction

While bacterial motility was discovered in 1683 by van Leeuwenhoek, who noted “many very small living animals, which moved very prettily” [2, p. 123], chemotaxis, the directed movement of bacteria toward attractant and away from repellent chemicals, was not described until the 1880s by Pfeffer [3] and Engelmann [4]. In the 1960s, the molecular basis of chemotaxis began to be elucidated starting with Adler and followed by Berg and colleagues, who explained how the biochemistry gives rise to the behaviour [5]. However, the early studies used *Escherichia coli* or *Salmonella enterica*, serovar typhimurium as model systems, whose biochemistry and behaviour is much simpler compared to other bacteria, as shown by Armitage and others later [6, 7, 8]. Recent years have seen another paradigm shift: the early notion that chemotaxis is metabolism-independent, also based on research in *E. coli*, proved not to be true [9, 10]. In this work, we try to explain the variety of behaviours seen in different bacteria. We argue that this requires us to consider chemotactic behaviours through the lens of the habitats the bacteria live in. Furthermore, we suggest a specific role for the metabolism-dependent behaviours in the early evolution of chemotaxis. Most importantly, we describe a new type of chemotactic strategy, called the “speculator” response, which is different from the paradigmatic “adaptive” response of *E. coli*. We show that the speculator response allows bacteria to co-localise with attractant and under some circumstances, it is as effective as the adaptive response. We present evidence suggesting that wild-type *Rhodobacter sphaeroides* uses the speculator response when grown under aerobic conditions.

This Chapter is organised in the following way: we start by briefly reviewing the numerous roles chemotaxis plays in various biological processes. We then discuss the different modes of bacterial motility and how chemotaxis relates to other types of taxis. We continue by describing the chemotactic behaviour, biochemistry and properties of the chemotactic response of *E. coli*, followed by a discussion of chemotaxis in other bacterial species. Last, we discuss previous research on chemotaxis evolution, thus setting up the stage for this work.

1.1 Chemotaxis in biological processes

Chemotaxis plays a role in the pathogenic behaviour of a number of bacteria. For example, chemotaxis helps *Helicobacter pylori*, one of the causative agents of peptic ulcers in humans, infect mouse hosts [11]. Likewise, virulence of *Pseudomonas aeruginosa*, an opportunistic human pathogen, was found to be attenuated in mice when one of the chemotaxis genes was mutated [12]. Furthermore, in *P. aeruginosa*, chemotaxis is involved in biofilm formation [13] and biofilms were implicated in a number of human [14] and plant [15] diseases, including cystic fibrosis, chronic bacterial prostatitis and periodontitis. Biofilms also pose problems for medical devices such as prosthetic heart valves, contact lenses and intrauterine devices [14]. *Agrobacterium tumefaciens* which causes crown gall disease in plants requires chemotaxis for pathogenicity in some types of soil [16].

Chemotaxis is also important in many processes in mammals. For example, it allows sperm to be guided to the egg [17]. Furthermore, chemotaxis is important in embryogenesis for the correct positioning of cells in the embryo [18]. Chemotaxis also guides axons during the development of the nervous system [19] and disruption of the neural migration leads to diseases such as schizophrenia, bipolar disorder and depression [20]. Chemotaxis is involved in the spread of cancer cells to healthy organs. Importantly, numerous drugs that target the chemicals attracting the metastasising cells are currently in use or undergoing clinical trials [21]. Chemotaxis also allows the cells of the immune system to patrol the body for foreign substances as well as travel to inflammation sites [22]. Some of the chemokines that act as attractants for the cells of the immune system have been implicated in HIV infection, multiple sclerosis and atherosclerosis [23].

Chemotaxis is also involved in symbiotic relationships between bacteria and animal or plant hosts. For example, bacteria facilitate nitrogen fixation in plants and are guided to plant roots by chemotaxis [24]. The bioluminescent bacterium *Vibrio fischeri* is assisted by chemotaxis in colonising a type of squid, preventing the squid from being seen by predators [25]. In the ocean, nutrients were traditionally considered to be distributed homogeneously due to water turbulence, making chemotaxis superfluous. However, recent developments show that this is not the case and marine bacteria do take advantage of chemotaxis. This may have implications for the rates of carbon, nitrogen and sulphur cycling in the ocean [26].

1.2 Types of motility and taxis

1.2.1 Motility

The major modes of active bacterial movement are swimming, swarming, twitching, gliding and actin-based motility. In liquid media, bacteria use swimming and movement is achieved by the rotation of flagella which act as propellers. Swarming, twitching and gliding are all surface-based types of motility [27]. While swimming is used by individual cells, swarming is a group behaviour and swarmer cells have more flagella per cell than swimmer cells (hyperflagellation). Twitching requires type IV pili which act as grappling hooks: they extend from the front of the cell, adhere to the surface and retract, pulling the cell forward. The definition of gliding has evolved over time; at present, gliding is defined as a type of surface motility that involves neither flagella nor pili. A recent review discusses the possible ways in which gliding could be achieved [28]. Actin-based motility is used by some intracellular microorganisms and involves the exploitation of the eukaryotic cytoskeleton for movement within and between eukaryotic cells [29].

1.2.2 Taxis

Chemotaxis is the best-studied member of a wider class of taxis behaviours. While in chemotaxis cells seek high attractant concentrations, in precision sensing cells localise at intermediate values [30]. This is the case in thermotaxis [31] and pH taxis [32]. Interestingly, in *E. coli*, pH taxis [32] and likely also thermotaxis [33, 34] are mediated by the same pathway that gives rise to chemotaxis. Osmotaxis may be similar to precision sensing in that cells are repelled by low and high concentrations of osmotic agents and attracted by intermediate levels [35] but this behaviour is much less understood. In magnetotaxis, bacteria sense Earth's magnetic field; in the Northern (Southern) hemisphere, bacteria move in the direction of the North (South) pole [36]. Depending on latitude, this may direct magnetotactic bacteria towards the ground. This allows bacteria to migrate nearly vertically in a water column, assisting them in the migration toward preferred oxygen concentrations (aerotaxis; see below) [37].

1.2.2.1 Energy taxis

Adler noted in the summary of his landmark 1969 paper that in *E. coli*, “[e]xtensive metabolism of chemicals is neither required, nor sufficient, for attraction of bacteria to the chemicals” [38, p. 1596]. For a long time, chemotaxis was therefore considered metabolism-independent. However, extensive evidence now suggests that metabolism-dependent chemotaxis (also referred to as energy taxis) may actually be quite widespread. In energy taxis, bacteria respond to their own metabolic state rather than responding directly to the concentration of attractant. For ex-

ample, in *E. coli*, fumarate, an intermediate in the citric acid cycle, has been shown to regulate flagellar rotation [39, 40]. In *Azospirillum brasilense*, chemotaxis to most attractants was found to be metabolism-dependent [41]. One of the signatures of energy taxis may be the fact that bacteria accumulate in regions of attractant optimal for growth rather than regions with the highest attractant concentration [10]. A case in point is *A. brasilense* which accumulates at low concentrations of oxygen optimal for nitrogen fixation [42].

Interestingly, aerotaxis and phototaxis are examples of both metabolism-independent and metabolism-dependent chemotaxis. In an archaeon *Halobacterium salinarum*, oxygen appears to bind directly to a transducer protein and mediates the attraction of cells to regions high in oxygen, suggesting metabolism-independent taxis [43]. On the other hand, evidence from *E. coli* [44, 45], *R. sphaeroides* [46] and *A. brasilense* [41] suggests that changes in oxygen concentration affect the electron transport chain, which in turn affects the chemotactic behaviour of the bacteria, providing examples of metabolism-dependent chemotaxis. In some cases, it was possible to pinpoint where in the electron transport chain the signal sensed by the chemotactic pathways originates: in *E. coli*, receptors Aer and Tsr sense changes in the redox state and proton motive force, respectively, and transduce the signals to the chemotaxis pathway [47].

In *Synechocystis* sp. PCC 6803, phototaxis appears to be metabolism-independent because bacteria respond to light intensity gradients rather than absolute light intensity (responding to absolute intensity may be more relevant when seeking light intensity optimal for growth [10]) and inhibitors of photosynthesis have no effect on the phototactic response [48]. Furthermore, phototaxis in this species may be mediated by a photoreceptor that senses light directly [49]. On the other hand, phototaxis in *R. sphaeroides* is dependent on the photosynthetic apparatus and is therefore metabolism-dependent [50].

Another example of energy taxis is redox taxis where chemicals in the environment surrounding bacteria affect the redox state of the electron transport chain [51]. As mentioned above, Aer receptor in *E. coli* senses changes in the redox state caused by changes in oxygen concentration [47]; this behaviour is therefore aerotaxis as well as redox taxis.

1.3 Chemotaxis in *E. coli*

1.3.1 Behaviour

Movement of bacteria in liquid media consists of swimming (running) in straight lines (subject to rotational diffusion) interrupted by tumbling, i.e. re-orienting in a new, nearly random direction (early studies also referred to tumbles as twiddles) [52]. It was established early on that bacteria are too small (on the order of micrometres) to sense a spatial attractant gradient, i.e.

the difference in attractant concentration between the front and back of the cell [53]. Instead, bacteria move through space and sense temporal attractant gradients: they compare the recent attractant concentration to an attractant concentration experienced some time ago and respond to the difference [53, 54]. To describe this response in *E. coli*, we define the tumbling rate, that is, the probability of initiating a tumble per short time interval. In the absence of changes in the experienced attractant concentration, the tumbling rate is constant. When the bacterium experiences an increase in attractant concentration, tumbling rate decreases, increasing the length of runs in the direction of increasing attractant. Upon a decrease in the experienced attractant concentration, tumbling increases, shortening runs in an unfavourable direction [52, 53]. The bacterium responds to a decrease in repellent concentration in the same way as it does to an increase in attractant concentration [55].

E. coli possesses 5–10 peritrichous (located randomly on the surface of the cell) flagella. Running and tumbling correspond to the two directions in which the flagella can spin. Counter-clockwise (CCW) spinning results in running while clockwise (CW) spinning causes tumbling. While spinning CCW, the flagella function in a highly coordinated manner, forming a bundle. Spinning CW disrupts the bundle structure, which causes tumbling [56].

1.3.2 Biochemistry

In this section, we describe how the chemotactic behaviour of *E. coli* is achieved biochemically. A decrease in attractant concentration reduces the number of attractant molecules bound to receptors. Low occupancy of receptors promotes the activity of CheA via interaction with CheW [57]. CheA phosphorylates CheY [57] which is directly involved in switching the rotation of the flagellar motor to clockwise, inducing tumbling [58]. Continued tumbling due to increased levels of CheY_p is prevented by the action of CheZ which dephosphorylates CheY_p [59]. This excitation branch of the pathway is complemented by an adaptation branch, together achieving temporal comparison of attractant concentration. The adaptation branch involves two enzymes, CheR and CheB, that methylate [60] and demethylate [61] the receptors, respectively. This makes the receptors more or less capable of promoting CheA's activity [62]. In addition, CheA upregulates CheB's activity [59]. In summary, when the bacterium experiences a decrease in attractant concentration, tumbling is induced via CheA (through the excitation branch), but CheA also increases CheB's activity resulting in demethylation of receptors, which in turn downregulates CheA, returning the tumbling rate to basal levels (through the adaptation branch). Crucially, methylation and demethylation are both slower than the other reactions [54]. As a consequence, it is the interplay of two factors, receptor occupancy by attractant molecules (that represents the current attractant concentration), and receptor methy-

lation level (representing the past attractant concentration), that determines the tumbling rate. The resulting chemotactic response is referred to as the adaptive response after the relaxation of the tumbling rate (adaptation) that follows the initial peak response (excitation). Interestingly, the tumbling rate relaxes exactly to pre-stimulus levels after the attractant concentration stops changing [52, 53, 55], exhibiting “perfect”, “precise” or “exact” adaptation. The time it takes for the tumbling rate to relax is referred to as the adaptation time.

1.3.3 Properties of the chemotactic response

The receptors of *E. coli* can detect minute differences in attractant concentration: responses were observed to a one-molecule change in receptor occupancy [54] (more recent estimates show responses to 3nM changes in attractant concentration [63]). Furthermore, *E. coli* shows high response sensitivity: an increase in receptor occupancy of 0.1–0.2% results in a transient 10% decrease in the tumbling rate [54], corresponding to a 50- to 100-fold amplification. Note the subtle difference in the two kinds of sensitivity: first, the *receptors* are sensitive in that they can detect small changes in attractant concentration. Second, the *response* is sensitive meaning that small changes in attractant concentration lead to large changes in the tumbling rate. (The molecular basis for *response* sensitivity is discussed in Section 3.1.) Bacteria have a wide “dynamic range”, that is, they can respond to changes in attractant concentration spanning multiple orders of magnitude; this is at odds with high response sensitivity: with a 100-fold amplification, the response should saturate for a 1% increase in receptor occupancy. However, it was shown that the methylation state of the receptors affects the response sensitivity and thus allows wide dynamic range [64, 65]. Furthermore, bacteria exhibit Weber’s law, i.e. they respond to relative rather than absolute changes in attractant concentration [66]. Related to this is the finding that bacteria respond to changes in the logarithm of attractant concentration [67, 68] and the ability of bacteria to perform fold-change detection [69].

In genetically identical cells, some aspects of the chemotactic response (adaptation time, steady-state tumbling rate) are found to vary on a cell-to-cell basis, while others (precision of adaptation) stay uniform or robust [70, 71, 72]. Stochasticity in protein expression levels affects the numbers of protein members of the chemotactic pathway, explaining the observed variation in adaptation time and steady-state tumbling rate [70]. On the other hand, topology of the chemotactic pathway [71] (established to be the “minimal topology providing high robustness” [73, p. 507]) and translational coupling of genes encoding the pathway [74] are thought to be responsible for robust perfect adaptation. Furthermore, it has been shown that robust perfect adaptation is encoded via integral feedback control [75].

Adaptation time and steady-state tumbling rate may be variable for a reason. Adaptation

time is equivalent to memory length, i.e. how far back in the past the bacterium “remembers” attractant concentrations. Longer memory is less sensitive to fluctuations in attractant concentration as it is easier to make out the general trend over a longer period of time (longer memory therefore acts as a low-pass filter [76]). However, longer memory may also make the cell respond to past attractant concentrations that are no longer relevant [70, 77, 78]. In a changing environment, it might be advantageous for a bacterial population to be heterogeneous in memory length [70, 78, 79] as this would result in bet-hedging ensuring that some members of the population always perform well, regardless of the specifics of the environment [80]. As for the steady-state tumbling rate, research indicates that keeping CheR expression at low levels would cause higher CCW rotation and longer runs, allowing the cells to explore their environment more efficiently [81, 82].

1.4 Chemotaxis in other bacteria

1.4.1 Behaviour

While some bacteria exhibit the same chemotactic behaviour as *E. coli*, responses of other bacteria differ. *S. typhimurium* [83] and *Bacillus subtilis* [84] are both examples of bacteria whose responses are very similar to that of *E. coli*. *R. sphaeroides* also shows the adaptive response (although see below) but its tumbling mechanism is different: while *E. coli* possesses multiple bidirectional flagella and tumbling is caused by their CCW rotation, *R. sphaeroides* possesses a single unidirectional flagellum and tumbling is due to Brownian motion that follows when the flagellum stops rotating [85]. Flagella in *Sinorhizobium meliloti* are also unidirectional but tumbling is caused by slowing their rotation [86]. *Myxococcus xanthus* displays the adaptive response despite the lack of flagella and use of surface-based gliding motility [87].

Variability in the behaviour of individual cells in populations of *R. sphaeroides* was reported. In particular, durations of tumbles, running speeds and adaptation times (some cells did not adapt at all) appeared to be more variable in *R. sphaeroides* [88] than in *E. coli* [52]. Interestingly, the aerotaxis receptor Aer of *E. coli* is not methylated and this appears to have no effect on the aerotactic efficiency as judged from swarm plates [89]. While a mechanism for methylation-independent adaptation has been proposed [89], it is also possible that adaptation is not actually required for successful chemotaxis. *A. brasilense* also exhibits methylation-independent aerotaxis [90].

Curiously, responses have been identified in which tumbling increases upon an increase in attractant. This appears to be the case in many mutant strains, such as aerotaxis [91] and redox taxis [51] in mutated *E. coli*, aerotaxis in mutated *S. typhimurium* [91], and phototaxis in mu-

tated Halobacteria [92]. In *S. typhimurium* chemotaxis, this alternative response can be caused by one of a number of single point mutations in the gene *cheU* that codes for a component of the flagellar motor switch [93]. In wild-type, aerobically-grown *R. sphaeroides*, this response was observed for a number of different attractants; crucially, bacteria exhibiting this response were capable of accumulating in regions with high attractant concentration [1]. *R. sphaeroides* contains 3 operons in its genome that encode chemotactic pathways [94]. Interestingly, the alternative response was also observed in anaerobically-grown bacteria in which operon 2 was deleted. In genetically-intact bacteria, this response is presumably masked by high levels of expression of operon 1 [95].

1.4.2 Biochemistry

Differences in chemotactic behaviour reflect differences in the underlying biochemistry. What can we then say about biochemistries of other bacteria? First, the same response does not necessarily mean the same biochemistry. As we mentioned in the previous section, response of *B. subtilis* is similar to that of *E. coli*. However, the network encoding the response is more complicated. For one thing, *B. subtilis* has two adaptation modules: one consists of the CheB-CheR pair and the other uses CheY feedback. In addition, the bacterium lacks CheZ and contains CheC, CheD and CheV which are not found in *E. coli* [84]. An analysis of prokaryotic genomes revealed that CheA, CheW, CheR, CheB, and the receptors belong to a set of core chemotactic proteins whereas the other proteins (the ones already mentioned and CheX) are “auxilliary” proteins—they are found in the genomes at a considerably lower frequency [96].

In a 2010 study, 61 out of 206 prokaryotic genomes were found to contain more than one of each of CheA, CheW, CheR, and CheB, suggesting that these bacteria have more chemotactic pathways. Furthermore, analysis of the genomes demonstrated that sets of genes may be clustered into operons [97]. Experimental results from *R. sphaeroides* support this hypothesis. The bacterium has 3 operons encoding 3 sets of chemotactic genes. Importantly, protein products of the third operon were reported to localise to the cytoplasm whereas products of operon 2 localise to the cell pole (as in *E. coli*) [98], providing further separation of pathways [97]. Moreover, as Table 2 in [87] shows, a number of other species have multiple chemotactic pathways. Interestingly, some chemotactic pathways appear to have been co-opted for functions other than chemotaxis. For example, *P. aeruginosa* has 5 clusters of chemotactic genes; cluster III has been implicated in biofilm formation [13] and cluster IV controls the production of type IV pili which are required for chemotaxis by twitching motility [99]. Furthermore, 2 out of 8 clusters in *M. xanthus* regulate developmental gene expression [87].

Bacterial species differ in the number of different types of receptors encoded in their

genomes. Interestingly, this number appears to depend on the bacterial lifestyles; while commensal bacteria such as *E. coli* have fewer receptors on average, bacteria that are found in multiple or more variable environments possess more receptors [100]. As discussed above, receptor clustering enables high response sensitivity in *E. coli* [65]. More recently, receptor clustering was found in a number of other bacterial species including *R. sphaeroides*, suggesting that high response sensitivity may be a more wide-spread phenomenon [101]. Consistently, the chemotactic response of *R. sphaeroides* was found to be very sensitive [102]. While in *E. coli*, receptors are embedded in the cell membrane, in other bacteria such as *R. sphaeroides* and *Vibrio cholerae*, receptors are also found in the cytoplasm [103, 104]. The cytoplasmic receptors interact with the products of the third chemotactic operon of *R. sphaeroides* [98] and could sense the metabolic state of the cell [103], providing metabolism-dependent chemotaxis in *R. sphaeroides*.

1.5 Evolution of chemotaxis

An aspect of chemotaxis which has not been studied in great detail is its evolution. There have been genomic analyses of chemotaxis [96] and flagellar [105, 106, 107] genes as well as more specialised analyses of genes coding for receptors [108, 100] and a class of phosphatases unrelated to CheZ of *E. coli* [109]. However, by design, these studies do not address the evolutionary pressures that shaped chemotaxis. Biochemical networks exhibiting the adaptive response of *E. coli* were evolved [110], but in this study, network performance was assessed by determining how closely the network output matches the adaptive response. A similar approach was used to evolve networks exhibiting perfect adaptation [111]. The issue with this type of approach is that it *starts* with the assumption that adaptive response or perfect adaptation are evolutionarily fit and *given* that assumption, networks generating these functionalities are evolved. In reality, evolution will favour any response that allows bacteria to co-localise with attractant and responses other than the adaptive response of *E. coli* may be possible. In a 2008 study, Goldstein and Soyer [112] used an approach that took this into account. In their simulations, network output regulated bacterial motility in a virtual world with an attractant distribution, and network performance depended on the ability of bacteria to find and stay in regions of high attractant concentration. They obtained networks encoding an “inverted” response in which the tumbling rate increases with increasing attractant concentration [112]. This is in contrast to the adaptive response of *E. coli* where tumbling is reduced when attractant concentration is increasing. By tumbling persistently in regions of high attractant concentration, virtual bacteria exhibiting the inverted response can co-localise with attractant efficiently [112]. The strength of this approach

lies in the use of a more realistic performance (fitness) criterion. A similar criterion was used in a more recent study where fitnesses of adaptive and inverted responses were analysed as a function of response sensitivity. The patterns in the fitness landscape suggested a particular role for response sensitivity in the evolution of chemotactic responses [113]. In this work, we build on the approaches advanced by [112] and [113], using realistic fitness criteria. In this work, we put forward a model that is evolutionarily yet more relevant, combining a realistic fitness criterion with a stochastic attractant distribution mimicking the kinds of environments bacteria may be expected to inhabit in the wild.

1.6 Aims

We ask two main questions in this work: why do different bacteria use different chemotactic responses and how has this diversity of approaches arisen? Chapters 2 and 3 address these questions in turn. In Chapter 2 we suggest that the efficacy of different chemotactic strategies may vary as a function of environment and bacteria inhabiting distinct environments may thus adapt to their respective environments by evolving different chemotactic strategies. To test this hypothesis, we optimise virtual bacteria with different chemotactic strategies under environments that differ in the way attractant is distributed in time and space. In Chapter 3 we attempt to identify relevant evolutionary pressures that shaped chemotaxis and possible evolutionary trajectories leading to the present-day diversity of chemotactic strategies. Building on the work of [113], we investigate the role of response sensitivity in this process.

Chapter 2

Optimal chemotactic responses in stochastic environments

2.1 Introduction

While *E. coli* has been instrumental for our understanding of chemotaxis, other bacteria show a considerable variety of chemotactic mechanisms and behaviours, as reviewed in Chapter 1. Perhaps the most perplexing is the observation that some bacteria tumble more in the presence of attractant. Interestingly, this behaviour was found in wild-type, aerobically-grown *R. sphaeroides* [1]. This response seems paradoxical, as the bacterium might be expected to run in the direction of decreasing attractant concentration and tumble more when it detects an increase in attractant concentration, leading to the accumulation of bacteria away from the attractant. In addressing these puzzling results, Goldstein and Soyer demonstrated the chemotactic efficacy of a non-adaptive “inverted” response [112, 113]. With this strategy, bacteria respond to the absolute attractant concentration, tumbling more and therefore maintaining their position in regions of higher attractant concentration. Although less effective than the adaptive response, the inverted response requires only low receptor sensitivity, and could function in the absence of effective receptors by coupling to the cell metabolism [114]. As we show, there are discrepancies between the inverted response and the response observed in aerobically-grown *R. sphaeroides*.

Why do different bacteria exhibit different chemotactic responses? One possible reason is that different bacteria have evolved for different environments. For example, while *E. coli* might be expected to inhabit a resource-rich environment, marine bacteria experience a harsh environment in which attractant is localised in short-lasting patches [115] with attractant concentration inside patches being 3 to 6 orders of magnitude higher than outside [26]. This has led to a number of marine-specific evolutionary adaptations such as higher running speed in *Pseudomonas haloplanktis* [116] and run-and-reverse (as opposed to run-and-tumble) chemotaxis in over 70% of marine bacterial species [117]. Unfortunately, most experimental and theoretical

studies to date consider chemotaxis in response to step functions or simple gradients [118], providing limited insights to how chemotaxis would function in different types of environments. In particular, there have been few studies [119, 120] analysing chemotactic strategies in stochastic environments, which are likely to be the most important environment during the evolution of a chemotactic response.

In this work we construct a model of a stochastic attractant distribution. By adjusting the manner in which attractant concentrations vary in time and space, the attractant distribution can mimic a range of environments that one might expect to find in nature. We use this model to study how performance and optimal properties of various chemotactic strategies vary as a function of environmental conditions. In particular, we describe a new type of chemotactic strategy called the speculator response. It differs from the adaptive response in that the tumbling rate increases with increasing attractant concentration; furthermore, the bacterium makes temporal comparisons of attractant concentration which distinguishes the strategy from the inverted response. We demonstrate the effectiveness of the speculator strategy and its remarkable match to the paradoxical response seen in wild-type, aerobically-grown *R. sphaeroides* [1].

2.2 Methods

2.2.1 Simulation overview

Our simulation is centred around a model of chemotaxis. Model parameters determine the characteristics of a chemotactic response displayed by a virtual bacterium. The bacterium moves in a one-dimensional virtual world containing a stochastic attractant distribution. Performance, or fitness, of a response, is equal to the average cell division rate, which we approximate as the inverse of the time it takes the bacterium to experience a specified amount of attractant. These components are combined in an optimisation framework which allows us to study the process of adaptive evolution of chemotaxis. The optimisation consists of a series of rounds of mutation and selection (generations). In the first generation, a “wild-type” chemotactic response is produced by initialising the model parameters randomly. A “mutant” response is subsequently generated by mutating one of the model parameters of the wild-type response. Fitnesses of the two responses are calculated and a Monte Carlo scheme is used to select one of the responses to pass on to the next generation where it serves as the wild-type.

2.2.2 Stochastic attractant distribution

The attractant distribution varies in both time and space. Two parameters, T (correlation time) and L (correlation length), determine the dynamics of the distribution. T is the timescale on which attractant concentrations change, while L determines the distance between peaks of at-

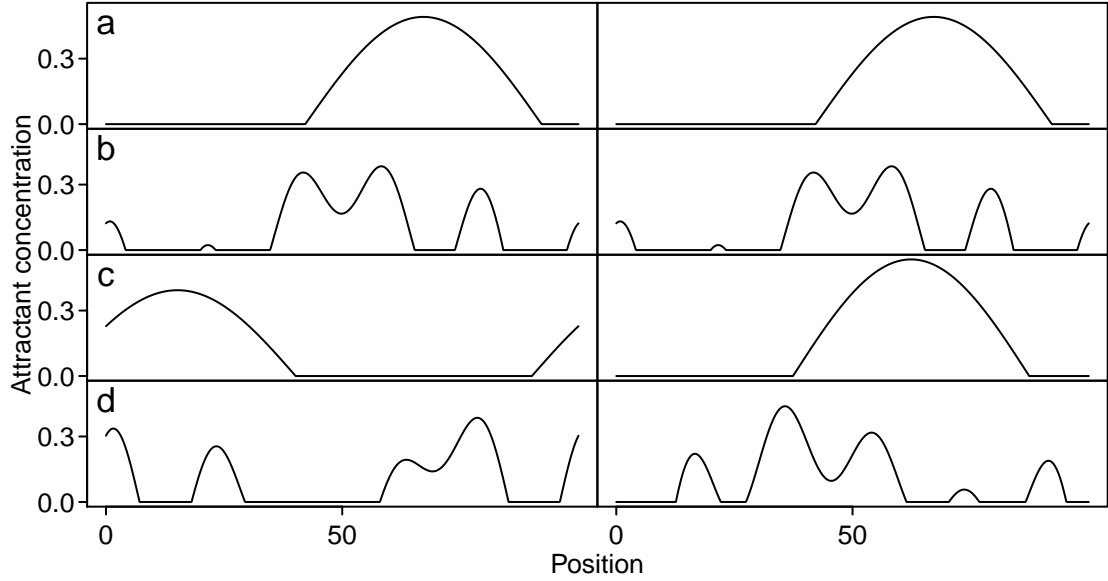


Figure 2.1: Examples of the stochastic attractant distribution at different combinations of T and L . Every row corresponds to a different combination. The left (right) panels show the distribution at time $t = 0$ ($t = 100$) in the simulation. a) $T = 10^4$, $L = 100$; b) $T = 10^4$, $L = 20$; c) $T = 100$, $L = 100$; d) $T = 100$, $L = 20$.

tractant concentration; the shorter L , the more numerous and narrow the peaks are and the shorter the distances between them. The average amount of attractant available in the world is independent of T and L . Figure 2.1 shows how the distribution looks at different combinations of T and L . Video A illustrates the distribution dynamics as a function of T and L .

We generate the attractant distribution by summing over cosine and sine modes with different mode numbers p so that the attractant concentration at time t and position x along the virtual world is calculated as

$$c(x, t) = \max \left(0, \sum_{p=1}^{p^*} X_p(t) \cos \left(\frac{2\pi p x}{l} \right) + Y_p(t) \sin \left(\frac{2\pi p x}{l} \right) \right) \quad (2.1)$$

where $X_p(t)$ and $Y_p(t)$ are stochastic weights, l is the length of the one-dimensional virtual world ($l = 100$) and $p^* = l/L$ is the largest mode included in the sum above. $X_p(0) = Y_p(0) = 0$ for all p s, and are updated at intervals of $\Delta t_c = T/100$ according to:

$$X_p(t + \Delta t_c) = X_p(t)(1 - \Delta t_c/T) + \eta_p(t) \sqrt{\frac{2\Delta t_c}{T p^*}} \quad (2.2)$$

where $\eta_p(t)$ is a white noise Gaussian random process ($\langle \eta_p(t) \eta_q(t') \rangle = \delta_{tt'} \delta_{pq}$), generated by a random number sampled from a normal distribution with mean 0 and variance 1. A similar expression is used for $Y_p(t + \Delta t_c)$. By construction, this results in a Markov process with

correlation time T and approximate correlation length $L = l/p^*$.

There are other functional forms possible for the attractant distribution. In particular, using a Gaussian function instead of sines and cosines might be more realistic as it is possible to model the process of attractant diffusion directly using Gaussian functions. The advantage of the current model is that, by construction, it allows the dynamics of the distribution to be finely tuned by adjusting the values of T and L . It is unclear whether such a model could be constructed as easily with Gaussian functions.

2.2.3 Chemotaxis

To model chemotaxis, we consider a single bacterium in a one-dimensional space with periodic boundary conditions. The bacterium can run to the left or right, or tumble. α and β denote the rates at which the bacterium starts and stops tumbling. While β is assumed to be constant, the basal rate α_0 is modulated by the chemotactic response of the bacterium to the experienced attractant concentrations. In particular, at time t ,

$$\alpha(t) = \max \left(0, \alpha_0 + \int_{-\infty}^t R(t-t')c(x_B(t'),t') dt' \right) \quad (2.3)$$

where $R(t)$ is the chemotactic response function [121] and $c(x_B(t),t)$ is the attractant concentration that the bacterium experiences at position $x_B(t)$ at time t . In contrast to [121], we do not assume deviations from α_0 to be small.

$$R(t) = (A/\tau + Bt/\tau^2) \exp(-t/\tau) \quad (2.4)$$

where τ controls the memory length, i.e. how far back in the past the bacterium “remembers” attractant concentrations, and A and B together determine the sensitivity and the characteristics of the response: adaptive, inverted, or speculator. In the adaptive response, A and B are constrained such that $A < 0$ and $B = -A$. This gives rise to a response function shown in red in Figure 2.2a that has a positive and a negative lobe. The red curve in Figure 2.2b illustrates the changes in α due to attractant addition and removal when a response function of this type is used. When $c(x_B(t),t)$ is increasing in time, such as when attractant is added, the negative lobe of $R(t-t')c(x_B(t'),t')$ has a larger area than the positive lobe, making the integral in equation (2.3) negative, leading to an α that is smaller than α_0 , resulting in a decrease in tumbling, as the red curve in Figure 2.2b shows at $t = 50$. The opposite happens when attractant is removed, resulting in an increase in tumbling at $t = 350$. The constraint $B = -A$ results in equal areas of the positive and negative lobes of $R(t)$, ensuring perfect adaptation and a basal

tumbling rate ($\alpha = \alpha_0$) for $50 < t < 350$. In the inverted response (Figure 2.2a, blue curve), $A > 0$ and $B = 0$, leading to a single-lobe response function. This results in a higher tumbling rate in the presence of attractant and a lower rate when attractant is absent, as the blue curve in Figure 2.2b shows. We also investigate a new type of response which we name the ‘‘speculator’’ response for reasons explained below. In the speculator response, $A > 0$ and $B < 0$, leading to a double-lobe response function (Figure 2.2a, green curve) that looks roughly like the negative of the adaptive response function (Figure 2.2a, red curve). This causes increased (decreased) tumbling when $c(x_B(t), t)$ is increasing (decreasing) in time (Figure 2.2b, green curve). The constraint of perfect adaptation is relaxed in the speculator response, so the areas of the positive and negative lobes are unequal (Figure 2.2a, green curve). This allows the steady-state α in the presence of constant attractant concentration to be different from α_0 , as shown for times $100 < t < 350$ (Figure 2.2b, green curve). The double-lobe response functions of adaptive and speculator response cause bacteria to make temporal comparisons of attractant concentration, while the lack of perfect adaptation in the inverted and speculator responses causes bacteria to respond to absolute attractant concentrations. Note that Figures 2.2a and 2.2b are purely illustrative; they do not reflect real or optimised responses.

Before a bacterium is introduced into the virtual world (at $x_B(0) = 0$), the attractant distribution is equilibrated for a period of at least T and α is initialised based on the equilibrated attractant distribution. The bacterium is then released and the state of the bacterium (whether it is running or tumbling) is updated every $\Delta t_B = \min(T, L/v, \tau/20)$ where v is the speed of the bacterium when running ($v = 1$). After $\alpha(t + \Delta t_B)$ is calculated using Equation (2.3), probability of tumbling ($p_T(t + \Delta t_B)$) or running ($p_R(t + \Delta t_B)$) is calculated, depending on whether the bacterium was running or tumbling previously. $p_T(t)$ can be found by solution of the following first-order differential equation for the two-state system of running and tumbling (note that α is used as a shorthand for $\alpha(t + \Delta t_B)$ below): $\frac{dp_T}{dt} = \alpha(1 - p_T(t)) - \beta p_T(t)$. The rate of change of $p_R(t)$ is equal to $-\frac{dp_T}{dt}$. We are interested in the solutions

$$p_T(\text{T}|\text{R}, t + \Delta t_B) = \frac{\alpha}{\alpha + \beta} (1 - \exp(-(\alpha + \beta)\Delta t_B)) \quad (2.5)$$

and

$$p_R(\text{R}|\text{T}, t + \Delta t_B) = \frac{\beta}{\alpha + \beta} (1 - \exp(-(\alpha + \beta)\Delta t_B)). \quad (2.6)$$

$p_T(\text{T}|\text{R}, t + \Delta t_B)$ is the probability of tumbling *given* that the bacterium was running previously; $p_R(\text{R}|\text{T}, t + \Delta t_B)$ is the probability of running *given* that the bacterium was tumbling previously. In a Monte Carlo scheme, these probabilities are used to decide whether the bacterium starts

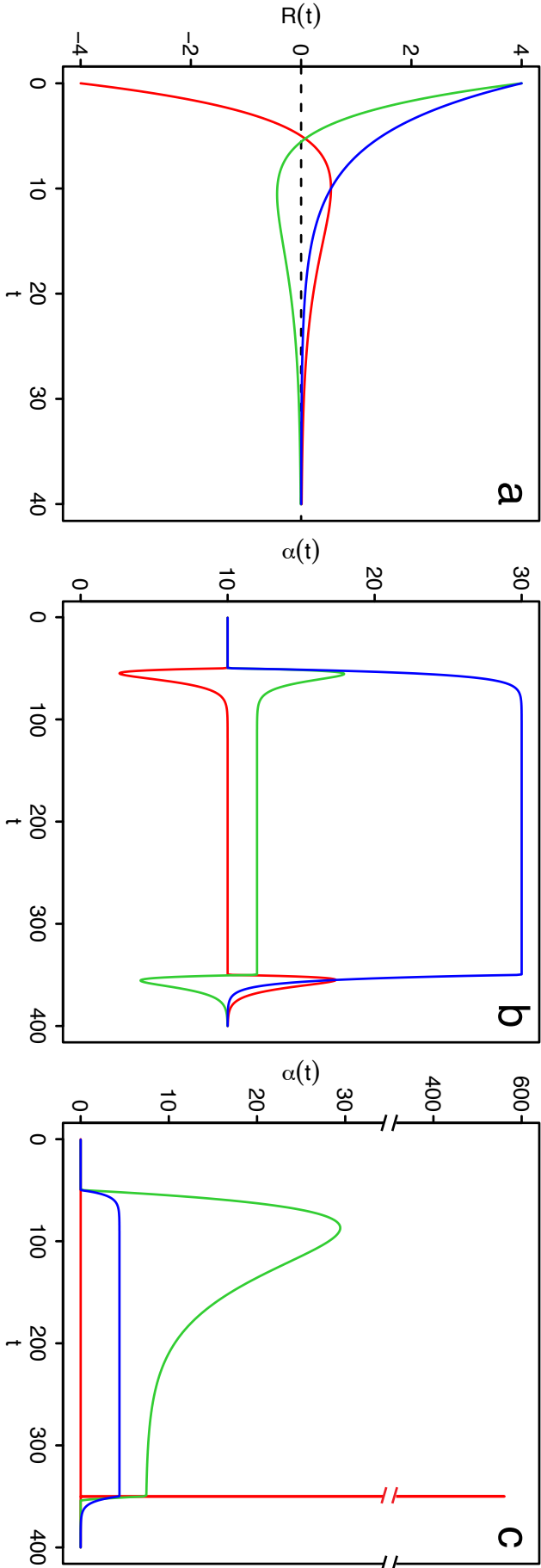


Figure 2.2: a) Illustrative examples of the response function for adaptive (red), inverted (blue) and speculator (green) response. The parameters used are $A = -20$, $B = 20$ and $\tau = 5$ for adaptive, $A = 20$, $B = 0$ and $\tau = 5$ for inverted, and $A = 20$, $B = -18$ and $\tau = 5$ for speculator response. b) Changes in α in response to step changes in attractant concentration for the responses from part a). $\alpha_0 = 10$ for all responses. Attractant (concentration of 1) is added at $t = 50$ and removed at $t = 350$. c) Changes in α in response to step changes in attractant concentration for adaptive (red), inverted (blue) and speculator (green) responses optimised for $T = 10^4$ and $L = 100$ ($\alpha_0 = 0.0084$, $A = -1500$, $B = 1500$ and $\tau = 0.020$ in the adaptive response, $\alpha_0 = 0.0063$, $A = 4.4$, $B = 0$ and $\tau = 5.0$ in the inverted response, and $\alpha_0 = 0.0089$, $A = 74$, $B = -67$ and $\tau = 33$ in the speculator response). Attractant (concentration of 1) is added at $t = 50$ and removed at $t = 350$. Note the change of scale on the y-axis.

tumbling or running given its previous state. Note that when the bacterium stops tumbling, it starts running left or right with equal probability.

Steady-state $p_T(T|R, t)$ and $p_R(R|T, t)$ can be obtained by setting $t = \infty$, giving:

$$p_T(T|R, t + \Delta t_B) = \frac{\alpha}{\alpha + \beta} \quad (2.7)$$

and

$$p_R(R|T, t + \Delta t_B) = \frac{\beta}{\alpha + \beta}. \quad (2.8)$$

2.2.4 Mutagenesis

In the first generation of the simulation, all response parameters are initialised randomly from a uniform distribution between 0 and 1 (but see below). In the adaptive response, only B is initialised and mutated, A is set to $-B$ (at $T = 10^4$, B is initialised between 1 and 10). In the speculator response, B is initialised randomly between 0 and -1 . In every generation, one response parameter is chosen at random and mutated. Parameters are mutated on a log scale by a transformation $\exp(\log_e(a) + r)$ where a is the parameter being mutated and r is a random number sampled from a uniform distribution between -0.2 and 0.2 . Further constraints on response parameter values are imposed for reasons of computational tractability: $\alpha_0 > 10^{-3}$ in adaptive and inverted response, $A > \exp(-1)$ and $|B| > \exp(-1)$ in speculator response, $\tau > 0.01$ in adaptive response.

2.2.5 Fitness

After mutagenesis, the fitnesses of responses described by the wild-type and mutant response parameters are determined. This is achieved by letting 10 identical wild-type and 10 identical mutant bacteria explore the virtual world with the stochastic attractant distribution. Each of the 10 wild-type bacteria is subjected to an attractant distribution initialised with a different random seed; the attractant distributions are then re-used for the 10 mutants. (As the attractant distribution is stochastic, estimates of response fitness are stochastic too. This scheme of competing the wild-type and mutant with the same attractant distributions is thus used to ensure that lucky mutants do not fix.) Each of the bacteria is run until it experiences $50T$ attractant units. $D_{w,i}$ ($D_{m,i}$) denotes the time it took the i -th wild-type (mutant) to experience the specified amount of attractant. Fitness of response $k = \{w, m\}$, F_k , is then calculated as $T \frac{1}{10} \sum_i \frac{1}{D_{k,i}}$.

2.2.6 Selection

Once fitnesses are determined, the probability of acceptance of the mutation, p_m , is calculated using the Metropolis-Hastings algorithm: $p_m = 1$ if $F_m \geq F_w$ and $p_m = \exp((F_m - F_w)/(UF_w))$

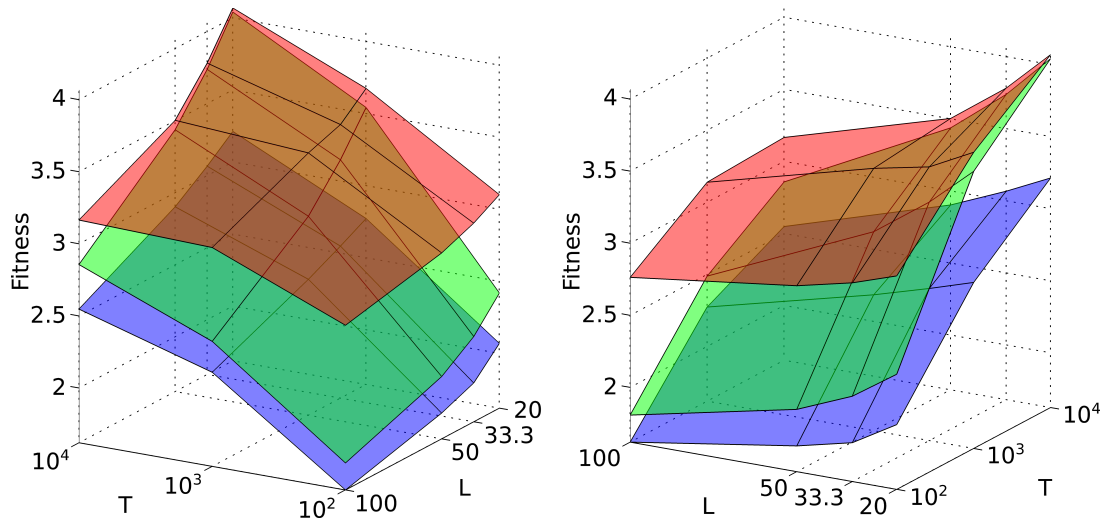


Figure 2.3: Fitness of adaptive (red), speculator (green) and inverted (blue) response as a function of T and L . The two panels show different views of the same plot. For each chemotactic strategy and combination of T and L , fitnesses are averaged over the last 600 generations of 3 replicate simulations.

otherwise. U , the temperature, is constant at 0.005. Simulations are run until the fitness stops increasing and stays constant for at least 600 generations. 3 replicate simulations are run for each chemotactic strategy and combination of T and L .

2.3 Results

2.3.1 Effects of environment on the chemotactic performance

The framework described in Section 2.2 allows us to assess the performance of a chemotactic response characterised by the response parameters α_0 , β , A , B and τ at a chosen combination of attractant distribution parameters T and L . This framework can be used to optimise the response parameters; any chemotactic strategy (adaptive, inverted, speculator) can be optimised by applying appropriate constraints on A and B .

Figure 2.3 shows the optimal fitnesses of adaptive, inverted and speculator responses as a function of T and L . Fitnesses are scaled by the fitness of a non-chemotaxing bacterium, whose fitness is independent of T and L : a bacterium with a relative fitness of 4 therefore takes 4 times less time to experience the same amount of attractant than a non-chemotaxing bacterium. In all strategies, fitness increases with increasing T and decreasing L . As T increases, attractant concentrations change more slowly, making it easier for bacteria to track attractant peaks. At shorter L , fitness is higher because there are more attractant peaks and they are closer to one another. This means that if a bacterium loses track of a peak, or a peak diminishes in amplitude over time, the bacterium only needs to travel a short distance to reach another peak.

We ensure that the total amount of attractant in the environment is independent of L . Although the total amount of attractant is different at different times during the simulation, we let the bacterium sample the environment long enough for the fluctuations to average out. The total amount of attractant is also independent of T when averaged over time. The dependencies of fitness on T and L in Figure 2.3 are therefore not caused by the total amount of attractant varying with T or L .

2.3.2 Speculator response

In addition to the previously studied adaptive and inverted responses, we characterise a novel chemotactic strategy. This “speculator” response, despite its seemingly paradoxical nature, is more fit under all studied conditions than the inverted response, although less fit than the adaptive response. Interestingly, at $T = 10^4$, $L = 20$, the fitness of the speculator response is nearly identical to the fitness of the adaptive response. To understand the mechanism of the speculator response, we consider the optimal values of response parameters (Table 2.1). The lack of perfect adaptation (optimal $|A| > |B|$) means that the bacterium will more often start to tumble when the attractant concentration is high, as shown in green in Figure 2.2c; the low value of β (Table 2.1) means that the bacterium will then continue tumbling, remaining in the region of high attractant. Consequently, the speculator response, like the inverted response (Figure 2.2c, blue curve), results in frequent long tumbles at high attractant concentrations. In contrast to the inverted response, the double-lobe response function of the speculator response results in a tumbling rate sensitive to the rate of change of the attractant. The long memory of the speculator response (large τ ; Table 2.1) allows sensitivity to long-term trends; this sensitivity, combined with the double-lobe response function, results in two important dynamical properties. Firstly, the bacterium compares recent attractant concentrations with a long-term average, tumbling more when the recent past is more favourable than the average, and therefore maintaining its position in regions of higher attractant concentration. Secondly, the bacterium is able to sense improving and worsening conditions at its current location. In particular, a decline in the attractant concentration results in a decrease in α , allowing the bacterium to swim away from a peak when conditions are changing for the worse. Swimming away leads to a further decrease in α , setting a feedback loop in motion, resulting in continued swimming until a new optimum is reached. The speculator response is therefore analogous to the behaviour of investors in financial markets: when the current performance is lower than the average, or when investment values are falling, speculators seek higher returns by abandoning their current position and investing elsewhere—hence the name “speculator” response. The behaviour of the speculator response, compared with the adaptive and inverted responses, is illustrated in Video B.

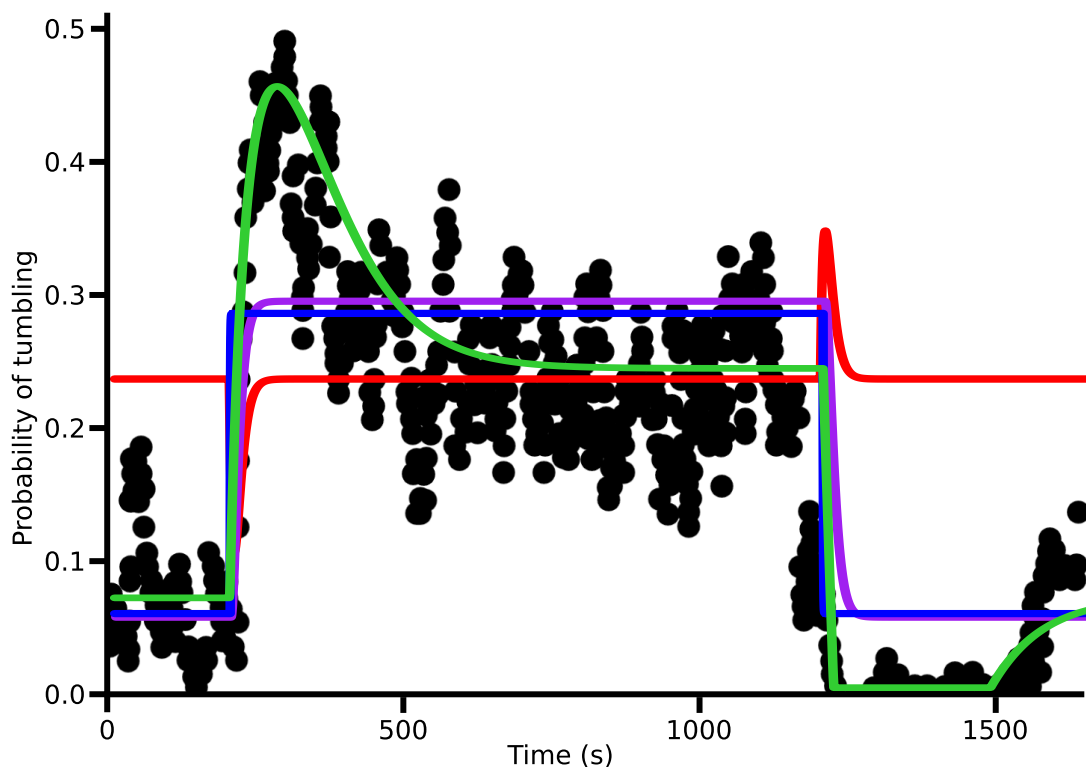


Figure 2.4: Curve-fit of our model of the speculator response (green curve) to the digitised data of [1] (black circles). Adaptive (red), inverted (blue) and delayed inverted (purple) responses are also fit to the data for comparison (the delayed inverted response is introduced in Chapter 3). The speculator response is described by the following response parameters: $\alpha_0 = 0.074 \text{ s}^{-1}$, $\beta = 0.034 \text{ s}^{-1}$, $A = 1300 \text{ mM}^{-1} \text{ s}^{-1}$, $B = -1000 \text{ mM}^{-1} \text{ s}^{-1}$ and $\tau = 71 \text{ s}$. Attractant is added at $t = 190 \text{ s}$ (at a concentration of 0.001 mM in correspondence to [1]) and removed at $t = 1200 \text{ s}$. The curve-fits were obtained by optimising the response parameters of the 4 responses to minimise the least-squares fits between the model and the digitised data. The data are digitised in MATLAB using the function `imfindcircles` [122].

Significantly, the time course of α in the speculator response closely matches the time course of probability of tumbling in aerobically-grown *R. sphaeroides* (see Figure 2A in [1]). Figure 2.4 shows a curve-fit of our model of the speculator response (green curve) to the digitised data of [1] (black circles). The closeness of the fit provides strong evidence that aerobically-grown *R. sphaeroides* uses the speculator response to respond to Na-succinate. Experimental results show that aerobically-grown *R. sphaeroides* performs well in swarm plates [1], demonstrating the efficacy of this response. Note that the speculator response provides a better fit to the data than the other responses. In particular, it predicts well how the probability of tumbling adapts after attractant is removed—both the initial dip in probability of tumbling and the adaptation that follows are predicted. We contacted the authors of [1] to obtain more recent data for fitting but no more data are available on this type of response.

2.3.3 Exploitation versus exploration in chemotaxis

As Figure 2.3 shows, at $T = 10^4$, $L = 20$, fitnesses of the adaptive and speculator responses are very similar despite the different mechanisms behind their chemotactic strategies. To better understand these strategies, we create a simple attractant distribution which consists of two Gaussians (at positions 25 and 75 in a world with a length of 100) oscillating in amplitude out of phase with each other: when one Gaussian is at full amplitude, the other has amplitude of zero. Amplitude, period of oscillation and width of the Gaussians are roughly matched to $T = 10^4$, $L = 20$ of the stochastic attractant distribution. For each of the two chemotactic strategies, we take a bacterium optimised for $T = 10^4$, $L = 20$ of the stochastic attractant distribution and simulate its movement in the virtual world with the two Gaussians. Figure 2.5 shows the mean position of the bacteria as a function of θ , the phase of the oscillations. Between $\theta = 0$ and $\theta = \pi/4$ the left Gaussian at position 25 is higher than the right Gaussian at position 75, but is decreasing. In the adaptive response (red curve), the bacterium is close to the top of this Gaussian during this period. The bacterium shows little movement toward the right Gaussian at position 75 until the right Gaussian is significantly higher i.e. $\theta > \pi/4$. In the speculator response (green curve), the bacterium cannot track the top of the Gaussian as well as in the adaptive response, as evidenced by the large standard deviation around position 25 (green shading). However, the bacterium more quickly adapts to the changing attractant levels, leaving the declining left Gaussian and moving toward the growing right Gaussian sooner.

The strengths of the adaptive and speculator responses therefore lie in exploitation and exploration, respectively. In the adaptive response, the bacterium can track the top of a peak efficiently while in the speculator response, the bacterium is better at leaving the declining peak and finding the increasing peak. The exploitation behaviour of the adaptive response is analogous to a hill-climbing algorithm, which efficiently finds, but may get stuck at, a local optimum. The exploration behaviour of the speculator response is more analogous to a Monte Carlo search algorithm in that the bacterium may leave a peak in search of a higher peak at the cost of its ability to track the peak top efficiently. This explains the trend in Figure 2.3: for large L , the number of attractant peaks is small, and exploiting a given peak is more important than exploring new peaks. Under these conditions, the adaptive response is significantly more effective than the speculator response. At short L , there are multiple peaks in the environment, each of which has a different amplitude. Under such conditions, the exploration behaviour of the speculator response allows the bacterium to locate higher peaks, while the exploitation behaviour of the adaptive response may lead to the bacterium tracking a suboptimal peak. At $T = 10^4$, $L = 20$, the two strategies are approximately equally effective, giving rise to very

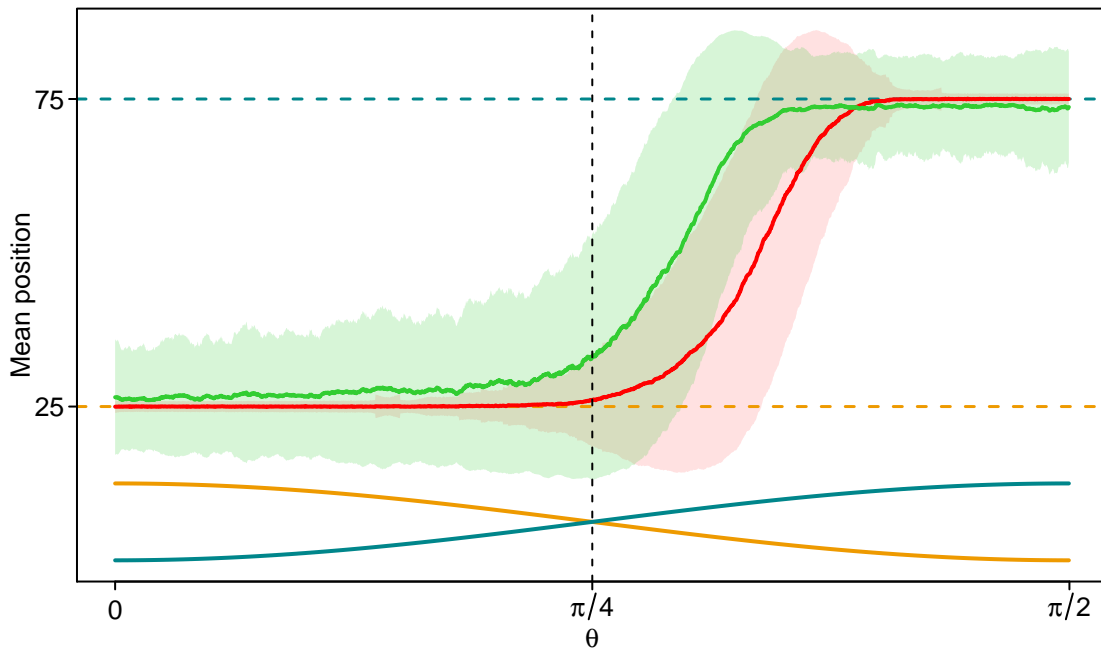


Figure 2.5: Mean position of bacteria performing adaptive (red curve) or speculator (green curve) response as a function of θ , the phase of the oscillations. Shading shows the standard deviation of the position. The Gaussians are centred at positions 25 (dashed gold line) and 75 (dashed turquoise line) and have a standard deviation of 3. Amplitudes of the Gaussians (not to scale, maximum amplitude is 1) are shown as a function of θ in the bottom part of the figure for the Gaussian at position 25 (gold curve) and 75 (turquoise curve). The Gaussians oscillate with a period $2\pi T$, with $T = 10^4$.

similar fitnesses (Figure 2.3).

2.3.4 Optimal response parameters and their dependence on T and L

2.3.4.1 Adaptive response

We next consider the optimal values of response parameters and how they depend on T and L . In the adaptive response, τ (the memory length) is very short (Table 2.1), allowing the bacterium to quickly adjust to small displacements from attractant optima. β , the rate at which the bacterium stops tumbling, is quite large, corresponding to short-lasting tumbles characteristic of chemotaxis in *E. coli* [52].

High sensitivity (large $|A|$ and $|B|$) is necessary for the bacterium to respond to small differences in attractant concentration characteristic of small displacements from the top of an attractant peak. High sensitivity is responsible for the high α when the attractant is removed at $t = 350$ in Figure 2.2c (red curve). Interestingly, optimal sensitivity is lower when T increases and L decreases (Figure 2.6); under these conditions, there are multiple peaks in the environment, each with a different amplitude. Lower sensitivity allows the bacterium to jump between peaks, decreasing the likelihood of getting stuck on a suboptimal peak. However, this is only beneficial at long T , when the peaks are stable over time. What is the source of the large standard deviations in Figure 2.6? First, let us note that the same fitnesses were reached in the 3 replicate simulations for a given combination of T and L , and fitnesses were stable over many generations (data not shown), suggesting two possible reasons for the large standard deviations: first, fitness may be unaffected by large variations in sensitivity. Second, a different optimal value of sensitivity in one of the replicate simulations could be compensated by a different optimal value of another response parameter in the same replicate. Further analysis could distinguish between these possibilities. These arguments hold for Figures in Section 2.3.4.2 as well, unless noted otherwise.

Optimal α_0 , the tumbling rate in the absence of attractant (or under constant attractant in case of perfect adaptation), is very low in all strategies, as is evident from Figure 2.2c and Table 2.1. Low α_0 enables bacteria to run persistently in order to find regions with more favourable conditions more quickly. The near-zero value of α_0 removes the possibility of α going below α_0 , eliminating the response to increasing attractant in the adaptive response (Figure 2.2c, red curve, $t = 50$).

2.3.4.2 Inverted response

In the inverted response, the bacterium tumbles more at higher concentrations of attractant (Figure 2.2c, blue curve). τ is longer than for the adaptive response (Table 2.1), allowing the

	τ	α_0	β	A	B/A
Adaptive	(0.072, 0.27)	(0.012, 0.062)	(10, 47)	(-11000, -5700)	-1
Inverted	(5.6, 8.3)	(0.0024, 0.0049)	(0.098, 0.68)	(2.0, 6.2)	0
Speculator	(39, 45)	(0.0030, 0.046)	(0.086, 0.44)	(47, 96)	(-0.85, -0.83)

Table 2.1: Range of optimal response parameters at $T = 10^3$, $L = 50$. 3 replicate simulations are run for each chemotactic strategy at $T = 10^3$, $L = 50$. For a given strategy and response parameter, mean values of the parameter are calculated separately in each replicate simulation by averaging the values of the parameter over the last 600 generations. Each range in the table is composed of the lowest and highest mean values obtained.

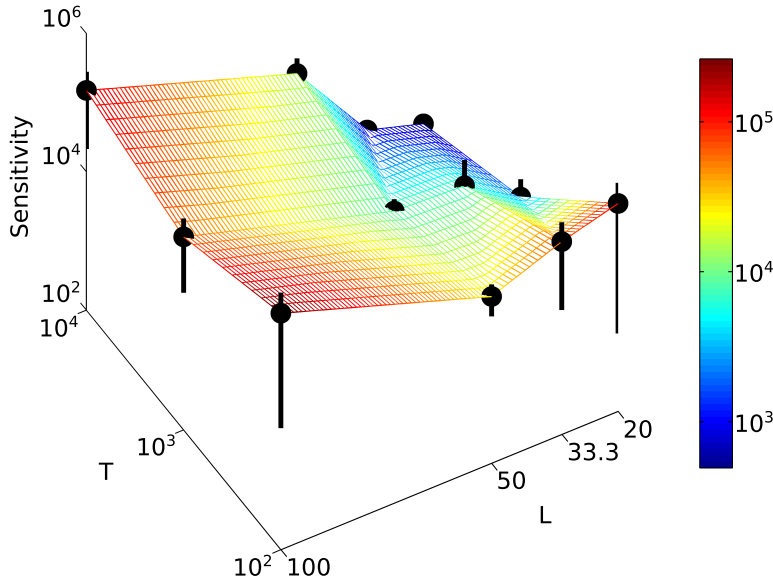


Figure 2.6: Sensitivity as a function of T and L in the adaptive response (note the log scale). Each data point is an average over the last 600 generations of 3 replicate simulations. Colour corresponds to the value of sensitivity (see the colour bar). The error bars show the standard deviation of the mean; they are asymmetrical because the data are plotted on a log scale.

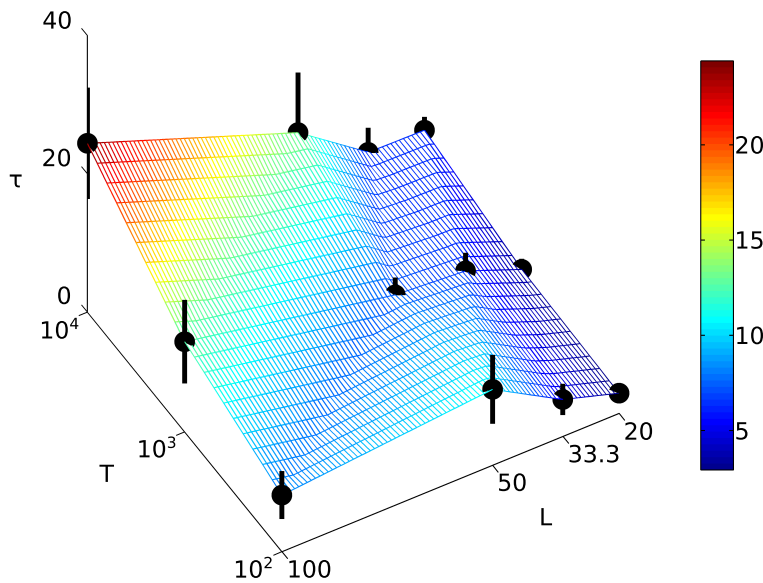


Figure 2.7: τ as a function of T and L in the inverted response. Each data point is an average over the last 600 generations of 3 replicate simulations. Colour corresponds to the value of τ (see the colour bar). The error bars show the standard deviation of the mean.

bacterium to integrate over short-term fluctuations. In both inverted and adaptive responses (Figures 2.7 and 2.8), optimal τ is lower when the attractant distribution varies rapidly in time (short T) or space (short L), otherwise bacteria respond to conditions that are no longer relevant. This is consistent with theoretical results showing that optimal adaptation time decreases for increasingly steep gradients [78, 79].

In both inverted and speculator responses, β is much lower than in the adaptive response (Table 2.1), resulting in significantly longer tumbles. This is central to the strategies, as it is the persistence of position when tumbling that allows bacteria to stay in regions of high attractant concentration. Furthermore, optimal β increases with increasing T in both inverted (Figure 2.9) and speculator (Figure 2.10) response, causing bacteria to be less persistent in maintaining their position when the attractant peaks are less stable in time. The peak at $T = 100$, $L = 100$

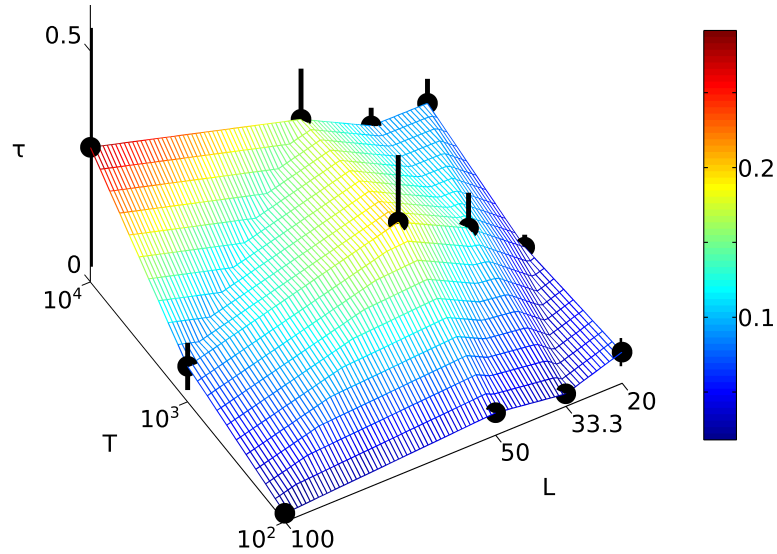


Figure 2.8: τ as a function of T and L in the adaptive response. See the caption of Figure 2.7 for more details.

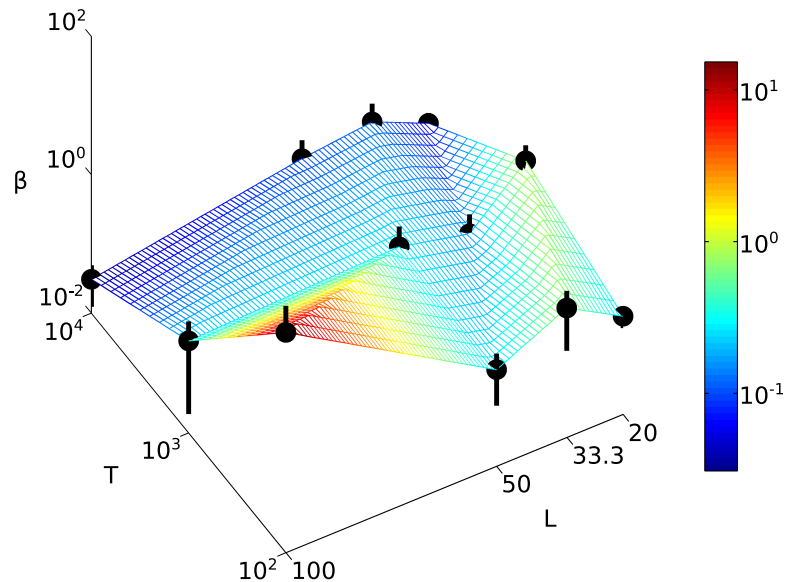


Figure 2.9: β as a function of T and L in the inverted response (note the log scale). See the caption of Figure 2.6 for more details.

in the inverted response is due to β reaching a higher optimum value in one of the replicate simulations (the fitness is the same as in the two remaining simulations). Interestingly, A is also higher in the same replicate simulation. Higher A leads to greater deviations of α from α_0 . Parallel increases in α and β likely leave $\frac{\alpha}{\alpha+\beta}$, the steady-state probability of tumbling (Equation (2.7)), unchanged. The steady-state probability of tumbling is therefore conserved in the 3 replicate simulations, providing an example of a compensatory change. The same reasoning likely applies to the peak at $T = 10^3$, $L = 100$ in the speculator response as both β and A are higher in one of the replicate simulations.

The sensitivity is lower than in the adaptive response (Table 2.1), in agreement with simple models showing that the inverted response is optimised by lower sensitivity [113]. Sensitivity needs to be tailored to the range of attractant concentrations the bacterium experiences: if it is too low, the bacterium will run past high concentrations of attractant; if it is too high, the

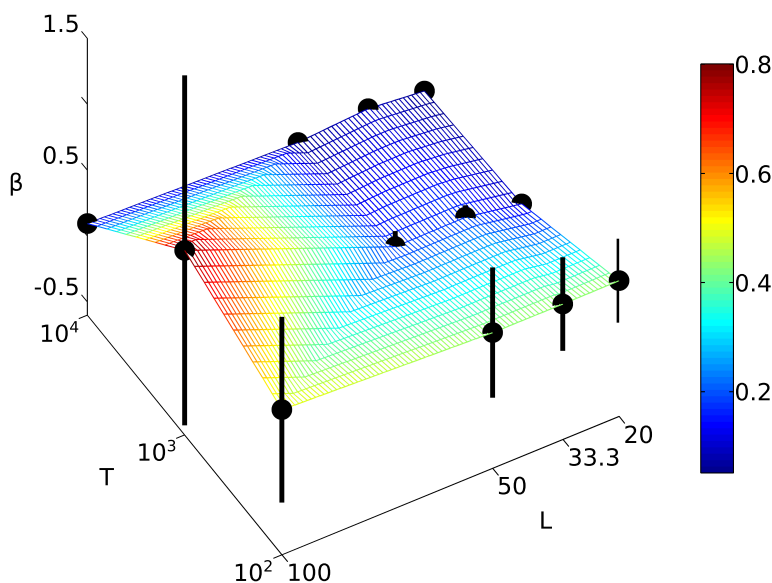


Figure 2.10: β as a function of T and L in the speculator response. See the caption of Figure 2.7 for more details.

bacterium will tumble at low concentrations of attractant, never reaching higher concentrations.

2.4 Discussion

In this work we describe a new chemotactic strategy, termed the speculator response, in which the bacterium compares the current attractant concentration with a long-term average; if the current concentration is higher than the long-term average, the bacterium tumbles persistently to maintain its position. On the other hand, declines in the current concentration will increase the probability that the bacterium will swim away to a higher peak. By considering stochastic attractant distributions, we show that under slowly-changing but spatially complex attractant concentrations (large T , small L), the speculator response is almost as efficient at co-localising with attractant as the adaptive response of *E. coli* (Figure 2.3). While the adaptive response achieves high fitness by accurately tracking the top of an attractant peak, the speculator response enables the bacterium to explore its environment and find higher peaks more efficiently (Figure 2.5).

The speculator response closely matches the response observed in wild-type, aerobically-grown *R. sphaeroides* (Figure 2.4). The optimised response parameters from our simulations are in arbitrary units, and cannot be directly compared with those obtained by the fit to the wild-type response (Figure 2.4). Interestingly, however, the ratio of B to A which quantifies the extent of departure from perfect adaptation ($B/A = -1$ corresponds to perfect adaptation) is similar between the optimised values obtained from the simulations and the response observed in aerobically-grown *R. sphaeroides* (-0.84 and -0.82 , respectively). Furthermore, we can acquire a rough estimate of the ratio of τ_S/τ_A (where τ_S and τ_A are the values of τ in the speculator and adaptive responses) by comparing the values of τ in aerobically-grown *R. sphaeroides*

(Figure 2.4) and wild-type *E. coli* [54]. This ratio ($71/1 = 71$) is of similar order of magnitude to the ratio for the optimised simulated responses ($43/0.20 = 215$), despite the multitude of differences between wild-type *R. sphaeroides* and *E. coli*.

The optimised adaptive response possesses high sensitivity (large $|A|$ and $|B|$; Table 2.1) consistent with experimental results from *E. coli* [123]. Furthermore, β , the rate at which the bacterium stops tumbling, is high, which is in line with the short tumbles observed in real bacteria [52]. In contrast to real bacteria, the optimised bacteria have a lower α_0 , and thus tumble less than real bacteria when attractant concentration is increasing (Figure 2.2c, red curve, $t = 50$). This may be an artefact of modelling chemotaxis in a one-dimensional environment: in a three-dimensional environment, tumbling may assist the bacterium in finding even steeper paths to attractant optima. We modelled chemotaxis as a one-dimensional process because of computational efficiency; the bacterium would take longer to sample a two- or three-dimensional environment sufficiently.

In this work we were by necessity confined to a relatively small range of T and L ; other conditions might exist (such as larger T and smaller L ; see Figure 2.3) that would favour the speculator response even more. Furthermore, our model does not take into account the motility-associated energy costs of the different chemotactic strategies. For instance, *R. sphaeroides* does not actively tumble, but rather stops running and lets Brownian motion generate the re-orientation, reducing the costs of strategies that involve longer tumbles [124]. The speculator response therefore might have emerged partly because *R. sphaeroides* uses rotational diffusion to achieve tumbling. Alternatively, rotational diffusion might have emerged in response to the bacterium using a strategy that involves long tumbles. It is unclear how relevant the energy costs of tumbling are as early calculations suggested the energy costs of chemotaxis to be negligible [125]. However, later research showed that while this is true for enteric bacteria, the energy costs are higher for marine bacteria because of their smaller size and higher swimming speed [126].

Our approach differs from that of other studies in that we consider realistic attractant distributions and extended tumbling times. The latter is essential for the speculator response to work as it allows bacteria to maintain their position in regions of high attractant concentration. Previous studies [127, 121, 128] modelled tumbles as instantaneous after chemotaxis in *E. coli* [52], however, experimental evidence from other bacterial species shows longer tumbling times [129, 85]. Our results add to the growing body of evidence that extended tumbles allow for emergence of other modes of chemotaxis [112, 113, 130].

Most studies to date considered chemotaxis in response to step functions or simple gradi-

ents [118]. While this is important for our understanding of the basic mechanisms of chemotaxis, we should recognise that chemotactic strategies were inevitably shaped by the environments the bacteria inhabited. For example, studies in marine bacteria unearthed specific adaptations to marine environments [119, 116, 117], highlighting the need to study chemotaxis in the context of realistic attractant distributions. Here, we propose a model of a stochastic attractant distribution which allows us to compare the performance of various chemotactic strategies under different environments and study how optimal properties of chemotactic responses change as a function of environmental conditions. This can also help us characterise the environmental conditions based on the strategies that have evolved. Further characterisation of natural environments [115] will allow theorists to construct more detailed attractant distributions and advances in microfluidics technologies will enable these environments to be reconstructed in laboratory settings [118].

Chapter 3

Response sensitivity as a driver for the evolution of chemotaxis

3.1 Introduction

The chemotactic response of present-day *E. coli* is very sensitive: an increase in receptor occupancy of 0.1–0.2% (corresponding to the binding of a single attractant molecule) gives rise to a transient 10% decrease in the tumbling rate [54]. This response sensitivity is achieved by signal amplification at the level of receptors [123] and the flagellar motor [131]. As predicted by models [132, 133] and later confirmed by experiments [134], receptors amplify the signal by interacting with one another in receptor clusters. Furthermore, CheB is likely to play a role [135] as response sensitivity is severely reduced in CheB mutants [123]. More recently, CheZ has been proposed as an alternative source of high response sensitivity [136]. Below, we refer to response sensitivity simply as sensitivity.

In Chapter 2 we showed that the optimal sensitivity is low (high) for the inverted (adaptive) response (Table 2.1). Consistent with our results, Soyer and Goldstein [113] showed that under low sensitivity, the inverted response is fitter than the adaptive response and under high sensitivity, the inverted response is less fit than the adaptive response. Based on these results, they formulated a scenario for the evolution of inverted and adaptive responses. As discussed above, the level of sensitivity depends on the molecular machinery. Crucially, Soyer and Goldstein argued that this machinery might be expected to improve over evolutionary time, enabling higher sensitivities. This would suggest that the inverted response evolved while sensitivity was still low, followed by the evolution of the adaptive response as sensitivity increased [113]. This scenario is especially attractive because the signalling pathway necessary to encode the inverted response may be simpler than that of the adaptive response [112]. In fact, the inverted response may be possible even without a dedicated signalling pathway by coupling the chemotactic response to cell metabolism: increased tumbling could be achieved by a metabolite binding to the

flagellar motor [114, 112, 113]; the concentration of the metabolite would serve as a measure of the environmental nutrient levels.

The scenario of Soyer and Goldstein presents an interesting problem. In the inverted (adaptive) response, the bacterium responds to a step increase in attractant concentration by a persistent increase (transient decrease) in tumbling; the evolutionary transition from inverted to adaptive response would therefore require a switch from increased to decreased tumbling (a “sign flip”) and a change of behaviour from persistent to transient. Could a single mutation achieve this? Alternatively, if multiple mutations are required, would the mutants be capable of co-localising with attractant? It has been shown that a single mutation in the *cheU* gene of *S. typhimurium* can achieve a sign flip, but the change in tumbling is transient [93]. Modelling work suggests that the amount of a signalling protein determines whether the dynamics of the protein concentration is persistent or transient [137] but additional mechanisms would likely be required to achieve sign flips.

How could the sensitivity-driven transitions between chemotactic responses be achieved? Soyer and Goldstein only considered inverted and adaptive responses; what is the role of the speculator response in the evolution of chemotaxis? In order to study these questions, we relax the response-specific constraints on the values of A and B . We find that two types of inverted response arise under low sensitivities: $A > 0, B \approx 0$ and $B > 0, A \approx 0$. In the latter case, the adaptive response ($A < 0, B > 0$) arises readily at higher sensitivities as the transition only involves a decrease in A . In the former case, we observe a transition to the speculator response ($A > 0, B < 0$) as this only requires a decrease in B .

Interestingly, nearly-perfect adaptation emerges in the adaptive response even without the constraint for perfect adaptation. Further analysis shows that perfect adaptation is optimal for the adaptive response; perturbing the adaptive response away from perfect adaptation by increasing the area of the positive or negative lobe leads to decreases in fitness.

3.2 Methods

We define sensitivity as $\sigma = \max(|A|, |B|)$. To model the constraints on sensitivity due to the limited amplification capabilities of the molecular machinery, we introduce $\sigma_M(g)$, the maximum value σ can take at generation g . We run long simulations (60000 generations) in which σ_M is initially low and constant ($\sigma_M(g) = 4$ for $1 < g < 10000$) and subsequently increases linearly (such that $\sigma_M(g) = 100$ at $g = 60000$). The initial value of $\sigma_M = 4$ corresponds to the typical optimal value of A in the inverted response (data not shown; Table 2.1 shows the range of the optimal value of A at $T = 10^3, L = 50$).

Response-specific constraints on A and B are relaxed to allow A and B to evolve freely, permitting transitions between responses as maximum sensitivity increases. To allow $a = \{A, B\}$ to mutate from a positive to a negative value (and vice versa) while still mutating it on a log scale, we define a threshold $h = \exp(-1)$. When a is positive (negative) and it is mutated below h (above $-h$), a becomes negative (positive). Specifically, a_{mut} , the mutated value of a , is calculated as $a_{\text{mut}} = \text{sgn}(a_{\text{log}} + r) \exp(|a_{\text{log}} + r| + \ln h)$ where $a_{\text{log}} = \text{sgn} a (\ln |a| - \ln h)$ and r is a random number sampled from a uniform distribution between -0.2 and 0.2 .

Apart from the changes discussed above, the optimisation proceeds as in Chapter 2; see the first paragraph of Section 2.2.1 for an overview.

3.3 Results

Unless otherwise noted, the results reported in this Chapter are for $T = 10^3$, $L = 50$; results for other combinations of T and L are qualitatively similar. “Simulations with unconstrained sensitivity” refer to the optimisations (under $T = 10^3$, $L = 50$) described in Chapter 2 (Section 2.3).

3.3.1 Transitions between responses due to changing response sensitivity

Figure 3.1 shows fitnesses and values of A , B and B/A as a function of evolutionary time for 3 replicate simulations (gold, turquoise and olive curves). In the “gold” and “turquoise” simulations, B equilibrates close to σ_M (dotted curve) during the low maximum sensitivity regime, while A becomes negative and smaller in magnitude than B . As $\sigma_M(g)$ increases (from $g = 10000$ onwards), we observe a transition to the adaptive response: B and A increase in magnitude, keeping their signs, and their ratio approaches -1 , indicating nearly perfect adaptation. In the “olive” simulation, $A > 0$ and B is negative and smaller in magnitude than A during the low σ_M . At higher σ_M , speculator response emerges as A and B increase in magnitude and their ratio approaches -0.82 , close to the range of the ratio observed in simulations with unconstrained sensitivity (-0.85 to -0.83 ; see Table 2.1).

While it is clear that adaptive and speculator responses arise under high maximum sensitivities, it is less apparent what the chemotactic strategies are of the responses observed at low σ_M . To better understand these responses, we plot their response functions (Figure 3.2a) and time-courses of α in response to attractant step functions (Figure 3.2b). Since in all 3 responses the optimal values of A and B are different from 0 and have opposite signs, all response functions are double-lobe (in the olive simulation, the negative lobe is extremely shallow due to the response function being “stretched” by a long τ). However, the areas of the positive lobes far outweigh the areas of the negative lobes. In the gold and turquoise simulations, this is due to $B > |A|$ (positive B encodes the positive lobe), while in the olive response it is due to $A > |B|$

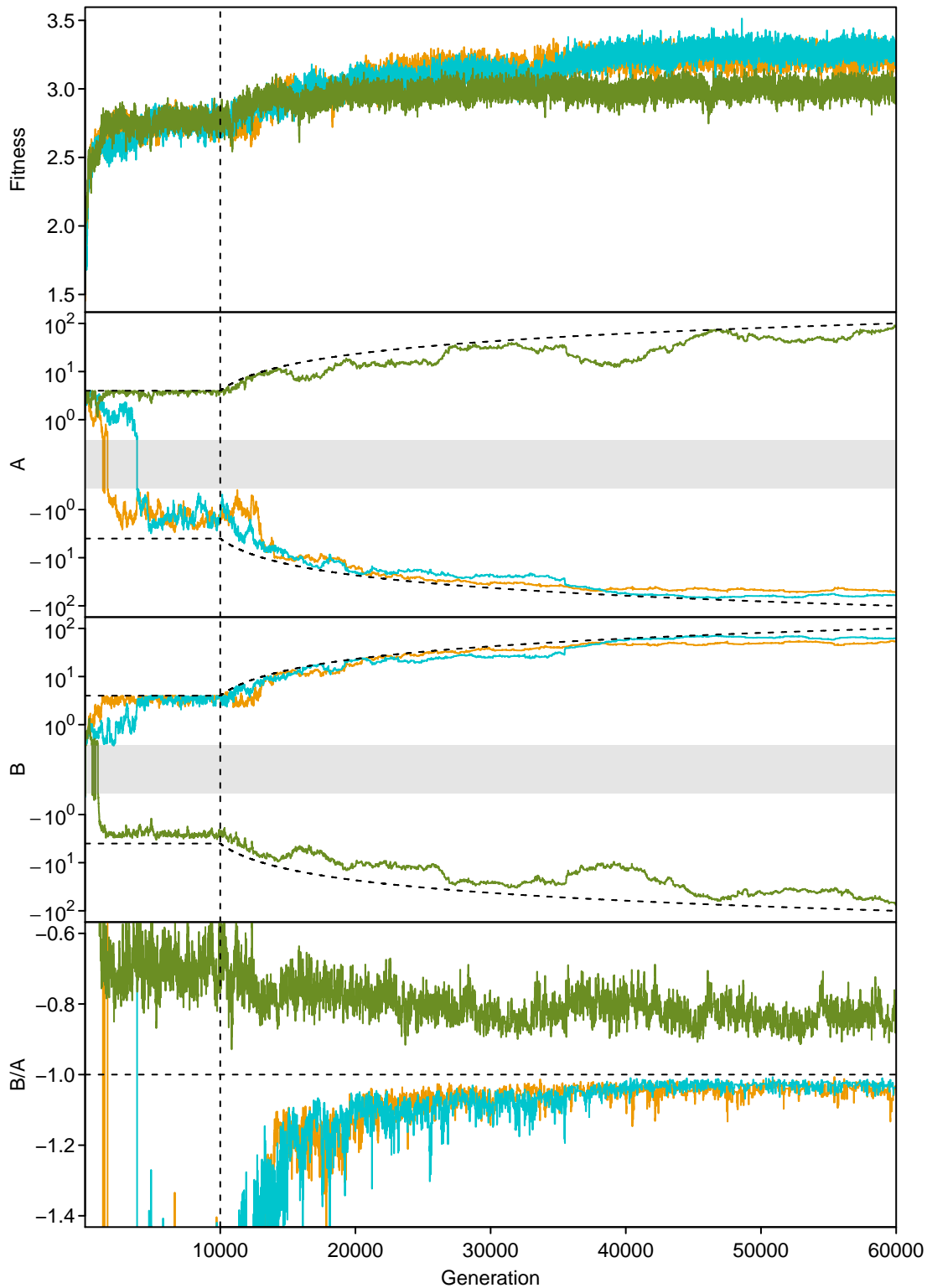


Figure 3.1: Fitnesses and values of A , B and B/A as a function of evolutionary time in 3 simulations (gold, turquoise, and olive curves). Note that A and B are plotted on a log scale. The grey shading in the plots of A and B spans vertically from $-h$ to h and represents the values at which A and B change signs (see Section 3.2). The dotted curves in the plots of A and B show $-\sigma_M(g)$ and $\sigma_M(g)$. The vertical dotted line running across all plots represents the generation in which $\sigma_M(g)$ starts increasing. The horizontal dotted line in the plot of B/A represents the value of B/A corresponding to perfect adaptation.

(positive A encodes the positive lobe). Because the response functions are dominated by the positive lobes, the modulation of α in the 3 responses is qualitatively similar to that of the inverted response: the bacterium tumbles more at higher concentrations of attractant, persisting in attractant-rich regions by virtue of extended tumbling.

The difference between the inverted responses encoded by positive A and positive B is that in the former, the response function gives the most recently experienced attractant concentrations the most weight ($R(t)$ is maximal at $t = 0$), while in the latter, the most weight is given to attractant concentrations experienced of order τ ago ($R(t)$ is maximal at $t = \tau$). We therefore refer to the inverted response encoded by positive B as the delayed inverted response.

To investigate the fitness of the delayed inverted response, we optimised it at different combinations of T and L by constraining A and B such that $B > 0$ and $A = 0$. Figure 3.3 shows the fitness of the delayed inverted response (purple surface) as a function of T and L ; fitness of the inverted response (blue surface; identical to the blue surface in Figure 2.3) is superimposed for comparison. The fitnesses of inverted and delayed inverted responses are very similar with delayed inverted response being slightly more fit. Although the difference is small, it is likely the reason why the delayed inverted response emerges more readily at low maximum sensitivities. Altogether, we ran 15 simulations with constrained maximum sensitivity (3 replicate simulations for each of 5 different combinations of T and L). In 13 simulations, the delayed inverted response arose at low maximum sensitivity, followed by a transition to the adaptive response at higher maximum sensitivities. In the remaining 2 simulations, the inverted response arose at low maximum sensitivity, leading to the emergence of the speculator response at higher maximum sensitivities. The fact that the speculator response only emerged in 2 out of 15 simulations suggests that it is less evolvable.

Note that we use a particular functional form for inverted and delayed inverted responses, given by Equation 2.4. However, other functional forms are possible and these should allow the types of transitions reported here, as long as they distinguish between “fast” and “delayed” inverted responses. In other words, despite the use of a particular functional form, our results should hold more generally.

3.3.2 Dependence of fitness and optimal response parameters on sensitivity

To better understand how sensitivity affects the performance and optimal values of response parameters in different chemotactic strategies, we optimised each strategy under a range of different fixed values of σ such that $B = \sigma$, $A = -B$ in the adaptive response, $A = \sigma$, $B = 0$ in the inverted response, $B = \sigma$, $A = 0$ in the delayed inverted response, and $A = \sigma$, B is unconstrained in the speculator response.

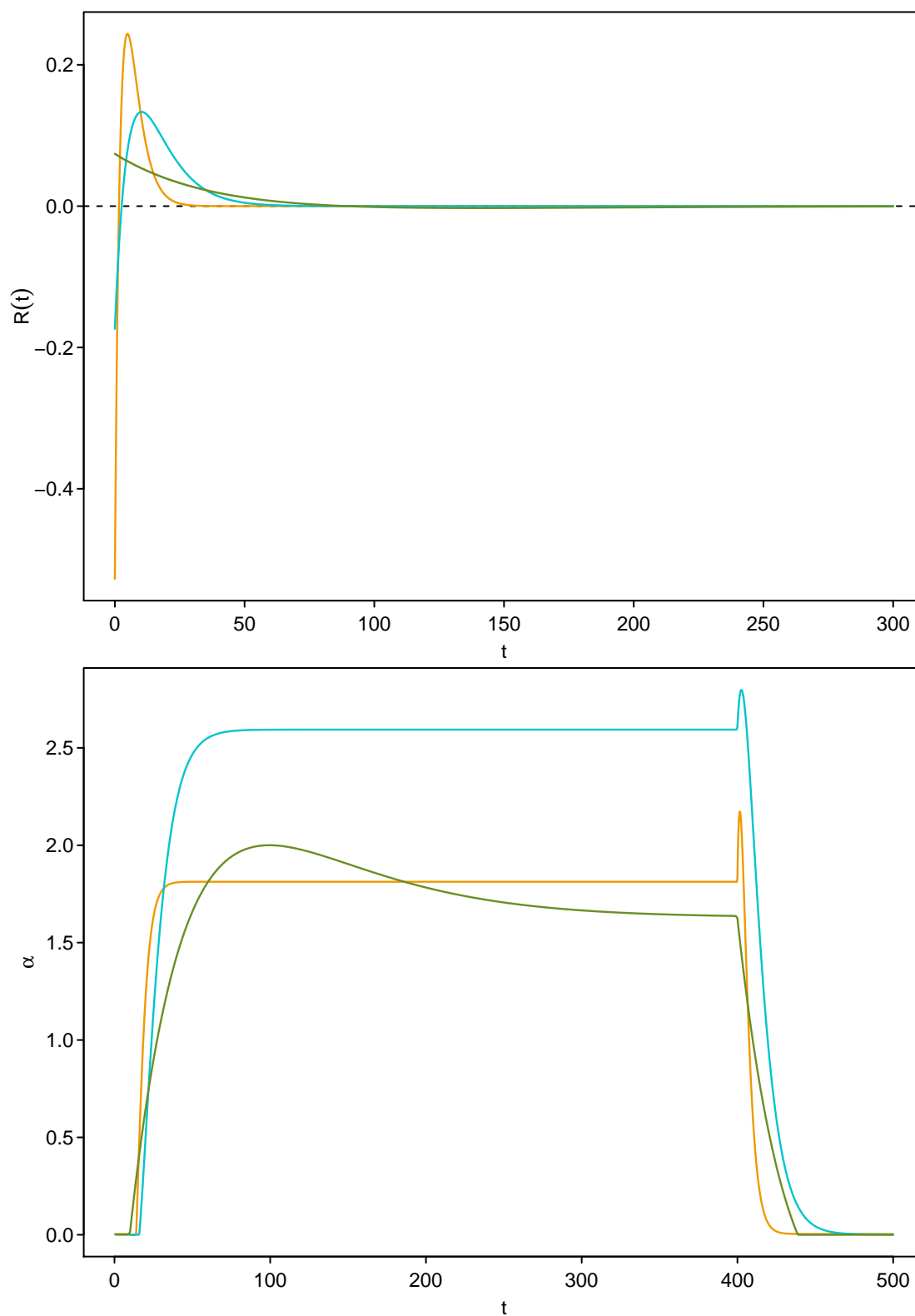


Figure 3.2: $R(t)$ (top) and $\alpha(t)$ (bottom) for responses from generation 10000 of the 3 replicate simulations from Figure 3.1 (the colour-coding is the same as in Figure 3.1). In the plot of $\alpha(t)$, 1 unit of attractant is added at $t = 10$ and removed at $t = 400$. The values of response parameters are $\alpha_0 = 0.0037$, $\beta = 0.15$, $A = -1.7$, $B = 3.5$, $\tau = 3.3$ in the gold, $\alpha_0 = 0.0012$, $\beta = 0.15$, $A = -1.3$, $B = 3.9$, $\tau = 7.7$ in the turquoise, and $\alpha_0 = 0.0013$, $\beta = 0.035$, $A = 3.8$, $B = -2.1$, $\tau = 51$ in the olive simulation.

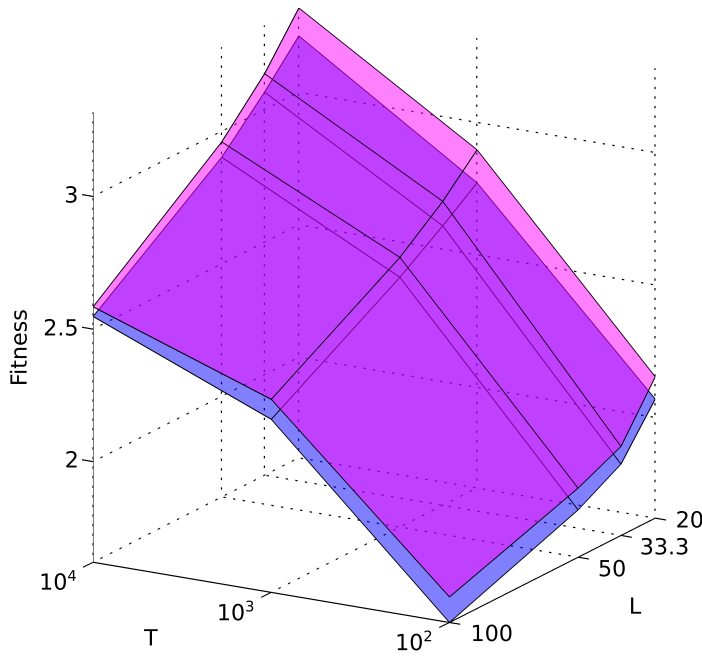


Figure 3.3: Fitness of delayed inverted (purple) and inverted (blue) response as a function of T and L . For each chemotactic strategy and combination of T and L , fitnesses are averaged over the last 600 generations of 3 replicate simulations.

Figures 3.4a, 3.4c and 3.4d show the fitnesses and optimal values of β and τ as a function of sensitivity for the different chemotactic strategies. Consistent with [113], inverted (blue) and delayed inverted (purple) responses are fitter than the adaptive response (red) under low sensitivity and less fit under high sensitivity. For $10 < \sigma < 28$, fitnesses of delayed inverted and adaptive responses are similar; interestingly, optimal values of β are very similar for the two responses at these sensitivities, and optimal values of τ are more similar for $\sigma \leq 28$ than for higher sensitivities. Importantly, similar optimal values of these parameters at similar values of sensitivity would make the transition between delayed inverted and adaptive responses more easily achievable.

At $\sigma = 1$, fitnesses of inverted and speculator responses are similar; above this sensitivity, the speculator response becomes the fitter strategy. Optimal β and τ are similar for the two responses at $\sigma = 1$, supporting the idea of an evolutionary transition between inverted and speculator responses near this sensitivity. As Figure 3.4e shows, the ratio B/A in the speculator response is closer to that observed in simulations with unconstrained sensitivity (dotted line) for $\sigma > 1$. At $\sigma = 1$, the magnitude of B/A is greater, meaning that the response function is dominated by the positive lobe encoded by positive A , as in the inverted response. Combined with the similar optimal values of β and τ and similar fitnesses, this means that the speculator response is in fact indistinguishable from the inverted response at $\sigma = 1$.

For a given strategy, each fitness value in Figure 3.4b was calculated by scaling the corresponding fitness value in Figure 3.4a by the maximal fitness obtained for that strategy in simulations with unconstrained sensitivity. A relative fitness of 1 means that the fitness is iden-

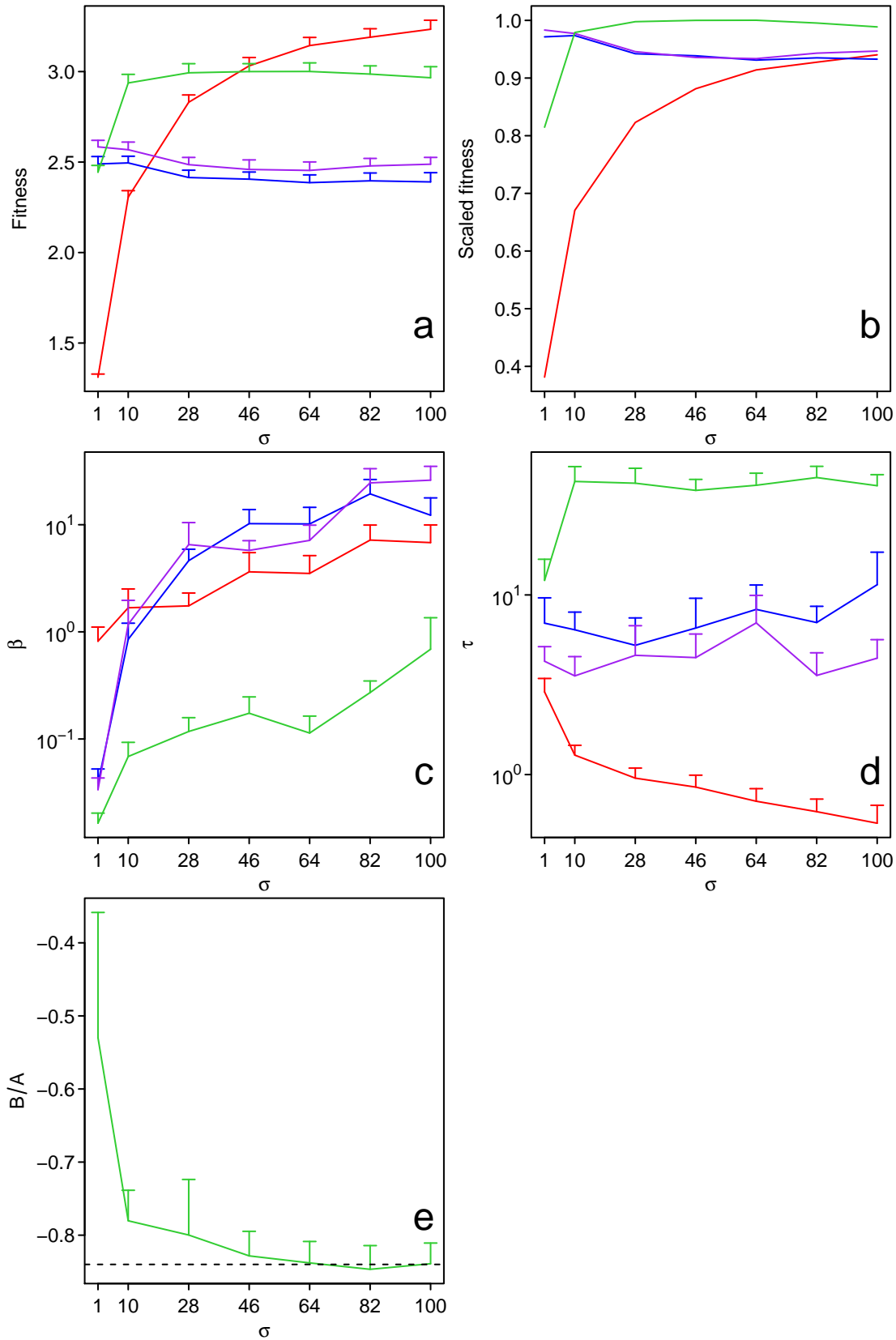


Figure 3.4: Fitness (a), scaled fitness (b), β (c), τ (d) and B/A (e) as a function of σ for adaptive (red), speculator (green), inverted (blue) and delayed inverted (purple) responses. Note that β and τ are plotted on a log scale. Each data point is an average over the last 300 generations of 3 replicate simulations. The error bars show the standard deviation of the mean.

tical to the maximal fitness. At $\sigma = 100$, the fitness of the adaptive response is at 90% of the maximal fitness, meaning that above a certain sensitivity, further increases in sensitivity only confer small fitness improvements, suggesting a flat fitness landscape. This likely explains why the standard deviation of sensitivity is extremely large in simulations with unconstrained fitness (Figure 2.6). In inverted and delayed inverted responses, fitnesses are very close to the maximal fitness for $\sigma \leq 10$, consistent with optimal sensitivities of 3.6 and 4.6 for the two responses obtained from simulations with unconstrained sensitivity. Interestingly, in contrast to [113], fitnesses do not deteriorate with increasing sensitivity, although they are slightly lower. We propose an explanation below.

We now consider the optimal values of response parameters in the different responses and how they depend on sensitivity. In the adaptive response, optimal β decreases with decreasing sensitivity, likely keeping the steady-state probabilities of tumbling in check: since the sensitivities studied here are lower than optimal sensitivities in simulations with unconstrained sensitivity (Table 2.1), the deviations of α from α_0 are smaller, leading to lower steady-state probabilities of tumbling ($\frac{\alpha}{\alpha+\beta}$; see Equation (2.7)). However, because β decreases in parallel to α , the steady-state probabilities of tumbling likely do not change. Keeping the steady-state probabilities of tumbling conserved is in the interest of the bacterium; when the probabilities are too low, the bacterium cannot respond to small changes in attractant concentration. This is particularly detrimental when the attractant concentration is decreasing: the concentration has to decrease sufficiently for a running bacterium to detect the decrease and respond by tumbling.

In the inverted response, optimal β increases with increasing sensitivity. Increasing sensitivity leads to increasing steady-state probabilities of tumbling, resulting in the bacterium tumbling persistently at low attractant concentrations, preventing it from reaching higher attractant concentrations. However, as β increases in parallel to sensitivity, the steady-state probabilities of tumbling are unchanged. This is likely the reason why increasing sensitivity does not diminish fitness. Optimal τ is higher for the inverted response compared to the delayed inverted response. This is because the positive lobe of the delayed inverted response reaches farther into the past, requiring a shorter τ .

3.3.3 Perfect adaptation

In the simulations with constrained maximum sensitivity (Section 3.3.1), the ratio B/A converges to a value close to, but lower than, -1 in the adaptive response (Figure 3.1), indicating nearly-perfect adaptation. Why is nearly-perfect adaptation optimal? As explained above, when sensitivity is limited, the bacterium cannot respond to small decreases in attractant concentration as the concentration has to decrease sufficiently for the bacterium to detect the decrease

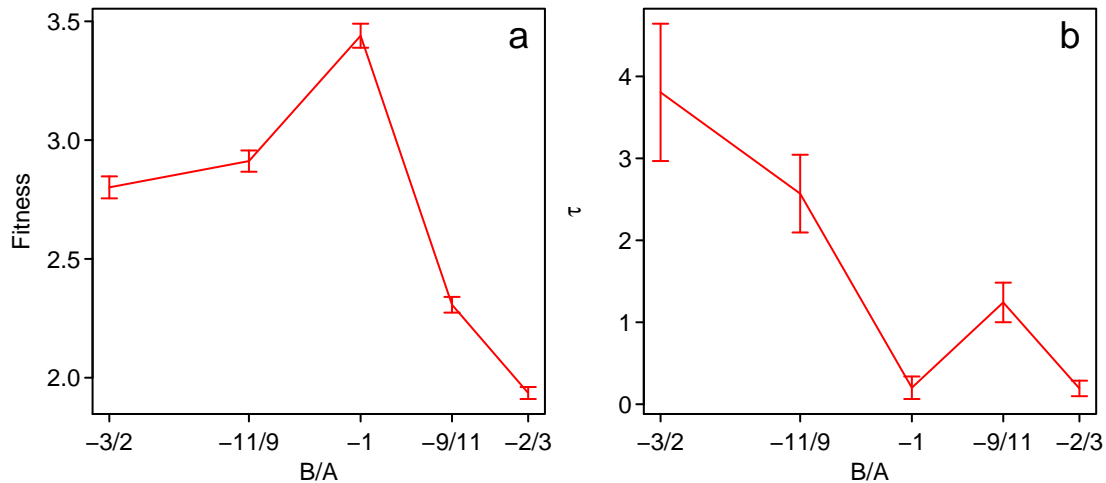


Figure 3.5: Fitness (a) and τ (b) as a function of B/A in the adaptive response. Each data point is an average over the last 700 generations of 3 replicate simulations. The error bars show the standard deviation of the mean.

and respond by tumbling. $B/A < -1$ means that $|A| < B$ which in turn means that the area of the positive lobe encoded by positive B is greater than the area of the negative lobe encoded by negative A . The response is therefore slightly biased toward tumbling, allowing the bacterium to terminate a run sooner when attractant concentration starts decreasing. Nearly-perfect adaptation is therefore optimal in this case. However, the effect is likely sensitivity-dependent: when sensitivity is higher, the bacterium can respond to small changes in attractant concentration and perfect adaptation may be optimal. This could be tested by optimising the adaptive response under different fixed values of maximum sensitivity and monitoring how the optimal value of the ratio B/A changes with maximum sensitivity (A and B would not be constrained in these simulations apart from the constrained sensitivity).

What are the effects of shifting the adaptive response away from perfect adaptation when sensitivity is not constrained? To answer this question, we optimised the adaptive response under different ratios of B/A ; the magnitudes of A and B were free to evolve as long as their ratio was constant. Figure 3.5a shows the fitness of the adaptive response as a function of the ratio B/A . Notably, fitnesses are higher for $B/A < -1$ than for $B/A > -1$. As explained above, at $B/A < -1$, the response function is dominated by the positive lobe encoded by positive B ; in fact, the higher the ratio B/A , the more the adaptive response resembles the delayed inverted response. This is further supported by the fact that at $B/A < -1$, optimal τ is greater than for the perfect adaptation case (Figure 3.5b), suggesting a shift toward the delayed inverted response.

At $B/A > -1$, the negative lobe encoded by negative A dominates and the bacterium is therefore biased toward running. This is not problematic as long as the experienced attractant concentration is increasing, as in this case, it is in the interest of the bacterium to suppress

tumbles and continue running in the favourable direction. However, the bias becomes an issue when the experienced attractant is decreasing: because of the bias, the bacterium does not tumble until the decrease in attractant concentration is sufficiently large to override the bias. As Figure 3.5a illustrates, this behaviour is less fit than the response for $B/A < -1$.

In the above analysis, the adaptive response was optimised for a particular value of B/A . How is the response fitness affected when B/A is perturbed in a response optimised under $B/A = -1$? As Figure 3.6 shows, perturbations lead to decreases in fitness. However, for $T = 100$, $L = 100$ (Figure 3.6d), fitness decreases much more steeply in response to perturbations than for other combinations of T and L ; interestingly, $T = 100$, $L = 100$ happens to be the combination of T and L for which the lowest fitnesses were reported in simulations with unconstrained sensitivity (Figure 2.3). Furthermore, fitnesses are only higher for $B/A < -1$ compared to $B/A > -1$ (i.e. the pattern seen in Figure 3.5a) for $T = 10^4$, $L = 20$ (Figure 3.6b) and $T = 10^3$, $L = 50$ (Figure 3.6c); for the remaining combinations of T and L , decreases in fitnesses are nearly symmetrical for $B/A < -1$ and $B/A > -1$. Further analysis would be required to understand the significance of these results.

3.4 Discussion

We propose a scenario for the evolution of the adaptive response of *E. coli* and the speculator response of *R. sphaeroides*. In this scenario, the response sensitivity is the main driver of chemotaxis evolution. In line with previous studies [113] we find that adaptive and speculator responses are fitter than delayed inverted and inverted responses under high sensitivity (Figure 3.4a). Importantly, high sensitivity was reported for both *E. coli* [123] and *R. sphaeroides* [102], and is also likely in other bacterial species given that receptor clustering, one of the major determinants of high sensitivity, appears to be a wide-spread phenomenon [101]. However, the molecular machinery that enables high sensitivity in present-day bacteria was either lacking or much less advanced in ancient bacteria, suggesting lower levels of sensitivity. Our results show that at low sensitivity, delayed inverted and inverted responses are fitter than the adaptive and speculator responses (Figure 3.4a). Consistently, we observed in our simulations the emergence of delayed inverted or inverted response under low sensitivity, followed by a transition to the adaptive or speculator response when sensitivity improved (Figure 3.1).

What evidence is there to support the emergence of delayed inverted and inverted responses early on during the evolution of chemotaxis? Previous studies showed that minimal pathways encoding these two responses are simpler than the pathway of the adaptive response of *E. coli* [112], suggesting that delayed inverted and inverted response may be more accessi-

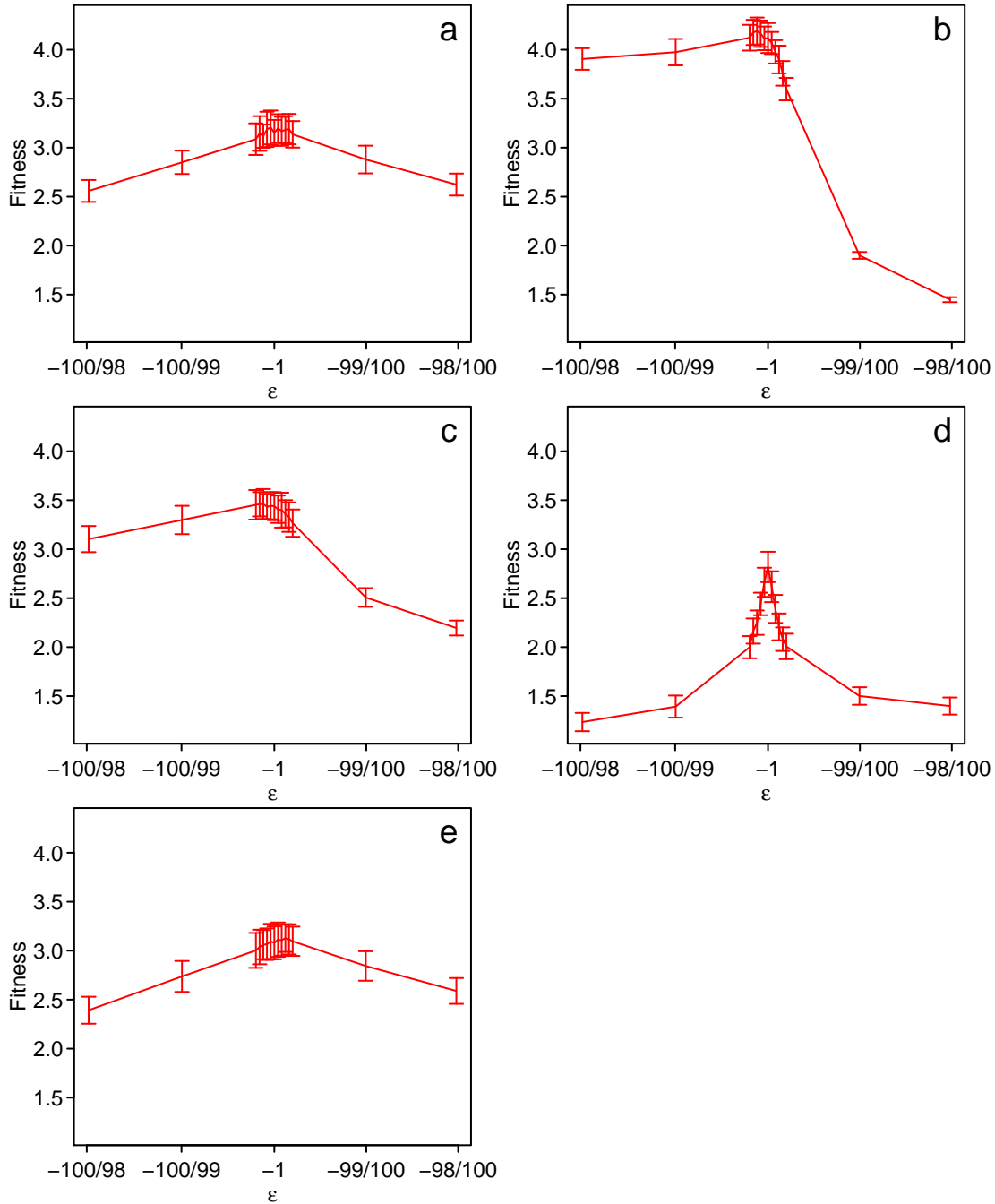


Figure 3.6: Fitness as a function of $\varepsilon = B/A$ in adaptive response (red curves) optimised under $\varepsilon = -1$ for a) $T = 10^4, L = 100$, b) $T = 10^4, L = 20$, c) $T = 10^3, L = 50$, d) $T = 100, L = 100$, and e) $T = 100, L = 20$. The response parameters for the adaptive responses optimised under $\varepsilon = -1$ are: $\alpha_0 = 0.016, \beta = 38, A = -290000, \tau = 0.20$ for $T = 10^4, L = 100$; $\alpha_0 = 0.0084, \beta = 54, A = -1500, \tau = 0.020$ for $T = 10^4, L = 20$; $\alpha_0 = 0.0094, \beta = 45, A = -3200, \tau = 0.050$ for $T = 10^3, L = 50$; $\alpha_0 = 0.0048, \beta = 86, A = -320000, \tau = 0.010$ for $T = 100, L = 100$; and $\alpha_0 = 0.0026, \beta = 61, A = -280000, \tau = 0.063$ for $T = 100, L = 20$. In the present analysis, given a particular combination of T and L and value of ε , $A_{\text{perturbed}}$ and $B_{\text{perturbed}}$ are calculated from B and ε as $A_{\text{perturbed}} = -B \left(1 - \frac{\varepsilon+1}{\varepsilon-1}\right)$ and $B_{\text{perturbed}} = B \left(1 + \frac{\varepsilon+1}{\varepsilon-1}\right)$. Fitness of a response characterised by $\alpha_0, \beta, A_{\text{perturbed}}, B_{\text{perturbed}}$ and τ is calculated as an average over 100 bacteria rather than 10 as in Chapter 2 (see Section 2.2.5). The error bars show the standard deviation of the mean.

ble by evolution than the adaptive response. Strikingly, the two responses could be achieved even without a dedicated pathway: a metabolite, or an attractant molecule taken up by the cell, could bind the flagellar motor directly, increasing tumbling [112, 114]. Fumarate, an intermediate metabolite in the citric acid cycle, has been shown to interact with the flagellar motor [39, 40], suggesting metabolism may regulate chemotaxis. Cellular metabolism likely occurs at timescales that are longer than timescales at which attractant concentration outside the cell changes [83], favouring the delayed inverted response which responds maximally to attractant concentrations experienced of order τ ago. Interestingly, optimal τ is higher for the delayed inverted response than for the adaptive response (Figure 3.4d), providing further support that the delayed inverted response could sense the metabolic state of the cell, while the adaptive response is optimised for sensing outside concentrations of attractant. Some attractants were found to be taken up by the cell [138]. Depending on the rates of transport across the cellular membrane, the direct binding of these attractants to the flagellar motor could bring about the inverted response which responds maximally to attractant concentrations experienced at present.

Delayed inverted or inverted response could provide a functional, although basic, chemotactic behaviour in ancient bacteria through sensing of the metabolic state of the cell or attractant uptake and binding to the flagellar motor. Once a basic strategy was in place, dedicated receptor and signalling proteins could be recruited that would encode the predecessor of present-day adaptive or speculator response. Possessing dedicated receptors could be advantageous as it might allow bacteria to distinguish between, and fine-tune their responses toward, different attractants. However, ancient receptors would only provide limited response sensitivities and the receptor-mediated responses would thus likely be of the inverted or delayed inverted type. Once the molecular machinery improved sufficiently, enabling higher sensitivity, the fitnesses of the adaptive and speculator responses would rise above those of the delayed inverted and inverted responses, and the adaptive or speculator response would become the preferred chemotactic strategy.

Evidence suggests that metabolic sensing could still be important in present-day bacteria. The most striking example is *A. brasilense* where metabolism is required for chemotaxis to most attractants [41]. In *R. sphaeroides*, chemotaxis to sugars requires metabolism [139]. A number of bacteria were found to possess cytoplasmic receptors [8]; in *R. sphaeroides* they were shown to cluster in a manner similar to that of the cell membrane receptors [104]. The cytoplasmic receptors could sense the metabolic state of the cell [103] and could also sense the concentrations of attractants that are taken up by the cell. Furthermore, some bacteria

harbour multiple chemotactic pathways [96]; in *R. sphaeroides*, some of these are targeted to the cytoplasm [98] and regulated independently [140], suggesting that they may sense the metabolic state of the cell through the cytoplasmic receptors. Last, enzymes involved in cellular metabolism were shown to interact with the flagellar motor [141, 142].

As pointed out by [114], the idea of metabolism-dependent chemotaxis is becoming fashionable again. Our results illustrate a possible role for metabolism-dependent chemotaxis in the evolution of chemotactic behaviour.

Chapter 4

Conclusion

The aim of this work was to investigate the observed diversity of chemotactic behaviours and identify evolutionary pressures that could have shaped chemotaxis.

In Chapter 2, we report a new type of chemotactic response termed the “speculator” response. We present evidence that this is the response used by wild-type, aerobically-grown *R. sphaeroides*. In this response, bacteria compare the current attractant concentration with a long-term average: when the current concentration is higher than the long-term average or is increasing, bacteria are likely to remain stationary by virtue of persistent tumbling. On the other hand, when the current concentration is lower than the long-term average, bacteria are more prone to running away in search of regions with higher attractant concentration.

The above results were obtained using a model of a stochastic attractant distribution; adjusting the manner in which attractant concentrations vary in time and space allows us to study the performance of the speculator response and the previously reported adaptive and inverted responses under different environments similar to those one might expect to find in nature. Our results show that all studied responses are fitter than a non-chemotaxing bacterium. The speculator response performs better than the inverted response regardless of the details of the attractant distribution. The adaptive response is fitter than the speculator response under most environments; however, when the attractant distribution is slowly-changing but spatially complex, fitnesses of adaptive and speculator responses are very similar. Further analysis shows that the adaptive response allows bacteria to track the top of an attractant peak efficiently (“exploitation”) but bacteria may get stuck at local maxima, whereas the speculator response allows bacteria to leave a peak when it is low or decreasing in amplitude (“exploration”) at the cost of the ability to closely track the top of the peak. Together, these results suggest that responses other than the adaptive response of *E. coli* allow bacteria to co-localise with attractant in a wide variety of environments. Furthermore, there are environments which favour certain types of responses over others, suggesting that the diversity of chemotactic behaviours observed in nature

could stem from different bacteria inhabiting distinct environments. Importantly, characterisation of natural environments will allow these predictions to be tested experimentally.

It is possible that the speculator response is fitter than the adaptive response in environments that are even more spatially complex than the environments studied in this work. This could be tested by including higher-order modes in the attractant distribution and determining the fitnesses of the two responses under a long correlation length. The differential energetic costs of active and passive tumbling likely also have an effect on response fitness. While in *E. coli* tumbling is an active process brought about by CW rotation of the flagellar motor, tumbling is passive in *R. sphaeroides*: the motor is stationary and the random re-orientation of the cell is generated by Brownian motion, suggesting a lower cost of tumbling in *R. sphaeroides* [124]. It would be interesting to incorporate tumbling costs in our model, which might lead to further increases in the fitness of the speculator response relative to the fitness of the adaptive response.

Our model is particularly amenable to studying the evolution of bet-hedging in the context of bacterial chemotaxis. Response fitness is currently calculated by subjecting 10 bacteria described by identical sets of response parameters to 10 different realisations of the stochastic attractant distribution. Rather than optimising response parameters directly, means and variances of individual parameters could be optimised instead. For each of the 10 bacteria, specific values of response parameters would be determined by sampling from distributions described by the associated means and variances. If the optimised variance of a particular parameter is large, it suggests that it is advantageous for the responses of the 10 bacteria to differ in the values of that parameter, indicating bet-hedging. This would allow us to explore various questions related to bet-hedging in bacterial chemotaxis: do some chemotactic strategies benefit from bet-hedging more than others? Which response parameters are subject to bet-hedging? Do some environments promote the evolution of bet-hedging more than others?

In Chapter 3, we propose possible routes for the evolution of adaptive and speculator responses. This evolution is driven by increases in response sensitivity that would occur over long evolutionary timescales [113]: response sensitivity is a function of the molecular machinery which likely improved over evolutionary time, giving rise to the high response sensitivity seen in present-day *E. coli* [65] and likely also other bacteria [101]. This process was simulated by constraining the maximum sensitivity and slowly raising the maximum. Under a low maximum sensitivity, inverted or delayed inverted response emerges. At higher maximum sensitivities, transitions from inverted to speculator and from delayed inverted to adaptive response are observed. At intermediate sensitivities, optimal response parameters for inverted/speculator and delayed inverted/adaptive responses are similar, aiding the transitions between the responses.

The notion that inverted-type responses emerged first during the evolution of chemotaxis is especially attractive because these responses could be achieved without a dedicated signalling pathway: an attractant molecule or a metabolite could bind the flagellar motor directly and increase the probability of CW rotation, thereby increasing the probability of tumbling. Together, these results suggest that response sensitivity could have acted as a driver for the evolution of various chemotactic strategies observed in present-day bacteria.

Interestingly, when the transition to the adaptive response occurred, the resulting adaptive response exhibited perfect adaptation, suggesting that perfect adaptation is the optimal state. We therefore explored the effects of perturbing the adaptive response away from perfect adaptation: indeed, the resulting fitnesses were lower. As reported in Chapter 2, the speculator response lacks perfect adaptation; it would be interesting to repeat the perturbation analysis on the speculator response, perturbing it further away and toward perfect adaptation.

How would the aforementioned evolutionary transitions be encoded biochemically? Biochemical networks encoding chemotactic responses were evolved previously; protein interactions were represented by rate constants and dynamics of the signalling pathway was described by a series of ordinary differential equations [112]. In the model, the activity of an effector protein (equivalent to the CheY protein in *E. coli*) represented the tumbling rate. We could therefore substitute the response function model currently in use for the biochemical network model of [112]. Constraining the maximum sensitivity could be achieved by capping the activity of the effector protein. Apart from potentially allowing us to study how the evolutionary transitions between inverted-type and adaptive and speculator responses could have occurred biochemically, this model could be used to study how environment affects biochemically-encoded chemotactic responses. In particular, a network optimised under one type of environment could be re-optimised under different types of environments by keeping the structure of the network intact but re-optimising the rate constants.

Appendix A

Dynamics of the attractant distribution

See video file `AppendixA.avi` on the enclosed CD (alternatively, clicking [this link](#) will take you to a YouTube video). Dynamics of the attractant distribution is shown for a) $T = 10^4$, $L = 100$; b) $T = 10^4$, $L = 20$; c) $T = 100$, $L = 100$; and d) $T = 100$, $L = 20$.

Appendix B

Dynamics of optimised adaptive, inverted and speculator responses

See video file `AppendixB.avi` on the enclosed CD (alternatively, clicking [this link](#) will take you to a YouTube video). Dynamics of a) adaptive, b) inverted and c) speculator responses are shown for $T = 10^4$, $L = 20$ (which is also the combination under which the responses were optimised). The parameters used are: $\alpha_0 = 0.0065$, $\beta = 4.2$, $A = -2100$, $B = 2100$, $\tau = 0.016$ in adaptive, $\alpha_0 = 0.0016$, $\beta = 0.048$, $A = 3.7$, $B = 0$, $\tau = 5.8$ in inverted and $\alpha_0 = 0.0089$, $\beta = 0.056$, $A = 74$, $B = -67$, $\tau = 33$ in speculator response. In the adaptive response, the bacterium swims up attractant gradients and tumbles when it experiences a decrease in attractant concentration. This leads to an oscillatory behaviour around peak maxima. In the inverted response, tumbling rate increases with increasing attractant concentration. Response sensitivity is optimised such that the bacterium tumbles most persistently at attractant concentrations which correspond to typical concentrations at attractant maxima. However, this means that the bacterium can get stuck at suboptimal concentrations on peaks that are larger than average by chance. The speculator response compares the current concentration of attractant with a long-term average. If the current concentration is greater than this average, the bacterium tumbles more. If the current concentration is lower than the average, or declining, the bacterium swims away, leaving the peak to search for higher attractant concentrations. The bacterium will typically run past peaks if their amplitude is lower than the peak it just left.

Bibliography

- [1] Helen L Packer and Judith P Armitage. Inverted behavioural responses in wild-type *Rhodobacter sphaeroides* to temporal stimuli. *FEMS Microbiology Letters*, 189(2):299–304, August 2000.
- [2] D Bardell. The roles of the sense of taste and clean teeth in the discovery of bacteria by Antoni van Leeuwenhoek. *Microbiological Reviews*, 47(1):121–6, 1982.
- [3] Wilhelm F P Pfeffer. Locomotorische Richtungsbewegungen durch chemische Reize. *Untersuchungen aus dem Botanischen Institut zu Tubingen*, 3:363–482, 1884.
- [4] Gerhart Drews. Contributions of Theodor Wilhelm Engelmann on phototaxis, chemotaxis, and photosynthesis. *Photosynthesis Research*, 83(1):25–34, January 2005.
- [5] Gerald L Hazelbauer. Bacterial chemotaxis: the early years of molecular studies. *Annual Review of Microbiology*, 66:285–303, January 2012.
- [6] George H Wadhams and Judith P Armitage. Making sense of it all: bacterial chemotaxis. *Nature Reviews Molecular Cell Biology*, 5(12):1024–37, December 2004.
- [7] Steven L Porter, George H Wadhams, and Judith P Armitage. *Rhodobacter sphaeroides*: complexity in chemotactic signalling. *Trends in Microbiology*, 16(6):251–60, June 2008.
- [8] Steven L Porter, George H Wadhams, and Judith P Armitage. Signal processing in complex chemotaxis pathways. *Nature Reviews Microbiology*, 9(3):153–65, March 2011.
- [9] Barry L Taylor, Igor B Zhulin, and Mark S Johnson. Aerotaxis and Other Energy-Sensing Behavior in Bacteria. *Annual Review of Microbiology*, 53:103–28, 1999.
- [10] Gladys Alexandre. Coupling metabolism and chemotaxis-dependent behaviours by energy taxis receptors. *Microbiology*, 156(Pt 8):2283–93, August 2010.

- [11] Karianne Terry, Susan M Williams, Lynn Connolly, and Karen M Ottemann. Chemotaxis plays multiple roles during *Helicobacter pylori* animal infection. *Infection and Immunity*, 73(2):803–11, 2005.
- [12] Steven Garvis, Antje Munder, Genevieve Ball, Sophie de Bentzmann, Lutz Wiehlmann, Jonathan J Ewbank, Burkhard Tummler, and Alain Filloux. Caenorhabditis elegans Semi-Automated Liquid Screen Reveals a Specialized Role for the Chemotaxis Gene cheB2 in Pseudomonas aeruginosa Virulence. *PLoS Pathogens*, 5(8):e1000540, August 2009.
- [13] Jason W Hickman, Delia F Tifrea, and Caroline S Harwood. A chemosensory system that regulates biofilm formation through modulation of cyclic diguanylate levels. *Proceedings of the National Academy of Sciences of the United States of America*, 102(40):14422–7, October 2005.
- [14] Rodney M Donlan and J William Costerton. Biofilms: survival mechanisms of clinically relevant microorganisms. *Clinical Microbiology Reviews*, 15(2):167–93, 2002.
- [15] Thomas Danhorn and Clay Fuqua. Biofilm formation by plant-associated bacteria. *Annual Review of Microbiology*, 61:401–22, January 2007.
- [16] Martha C Hawes and Laura Y Smith. Requirement for chemotaxis in pathogenicity of *Agrobacterium tumefaciens* on roots of soil-grown pea plants. *Journal of Bacteriology*, 171(10):5668–71, 1989.
- [17] Michael Eisenbach and Laura C Giojalas. Sperm guidance in mammals - an unpaved road to the egg. *Nature Reviews Molecular Cell Biology*, 7(4):276–85, April 2006.
- [18] Peter B Armstrong. The control of cell motility during embryogenesis. *Cancer and Metastasis Reviews*, 4(1):59–79, January 1985.
- [19] Duncan Mortimer, Thomas Fothergill, Zac Pujic, Linda J Richards, and Geoffrey J Goodhill. Growth cone chemotaxis. *Trends in Neurosciences*, 31(2):90–8, February 2008.
- [20] Manuel Valiente and Oscar Marin. Neuronal migration mechanisms in development and disease. *Current Opinion in Neurobiology*, 20(1):68–78, February 2010.
- [21] Evanthia T Roussos, John S Condeelis, and Antonia Patsialou. Chemotaxis in cancer. *Nature Reviews Cancer*, 11(8):573–87, August 2011.

- [22] Jose Luis Rodriguez-Fernandez and Laura Gomez Cabanas. Chemoattraction: Basic Concepts and Role in the Immune Response. *Encyclopedia of Life Sciences*, May 2013.
- [23] Tian Jin, Xuehua Xu, and Dale Hereld. Chemotaxis, chemokine receptors and human disease. *Cytokine*, 44(1):1–8, October 2008.
- [24] Lance D Miller, Christopher K Yost, Michael F Hynes, and Gladys Alexandre. The major chemotaxis gene cluster of *Rhizobium leguminosarum* bv. *viciae* is essential for competitive nodulation. *Molecular Microbiology*, 63(2):348–62, January 2007.
- [25] Cindy R Deloney-Marino and Karen L Visick. Role for cheR of *Vibrio fischeri* in the *Vibrio*-squid symbiosis. *Canadian Journal of Microbiology*, 58(1):29–38, January 2012.
- [26] Roman Stocker and Justin R Seymour. Ecology and physics of bacterial chemotaxis in the ocean. *Microbiology and Molecular Biology Reviews*, 76(4):792–812, 2012.
- [27] Rasika M Harshey. Bacterial motility on a surface: many ways to a common goal. *Annual Review of Microbiology*, 57:249–73, January 2003.
- [28] Beiyan Nan and David R Zusman. Uncovering the mystery of gliding motility in the myxobacteria. *Annual Review of Genetics*, 45:21–39, January 2011.
- [29] Marcia B Goldberg. Actin-based motility of intracellular microbial pathogens. *Microbiology and Molecular Biology Reviews*, 65(4):595–626, 2001.
- [30] Bo Hu and Yuhai Tu. Behaviors and strategies of bacterial navigation in chemical and nonchemical gradients. *PLoS Computational Biology*, 10(6):e1003672, June 2014.
- [31] Eli Paster and William S Ryu. The thermal impulse response of *Escherichia coli*. *Proceedings of the National Academy of Sciences of the United States of America*, 105(14):5373–7, April 2008.
- [32] Yiling Yang and Victor Sourjik. Opposite responses by different chemoreceptors set a tunable preference point in *Escherichia coli* pH taxis. *Molecular Microbiology*, 86(6):1482–9, December 2012.
- [33] Takafumi Mizuno and Yasuo Imae. Conditional inversion of the thermoresponse in *Escherichia coli*. *Journal of Bacteriology*, 159(1):360–7, July 1984.
- [34] Kayo Maeda and Yasuo Imae. Thermosensory transduction in *Escherichia coli*: inhibition of the thermoresponse by L-serine. *Proceedings of the National Academy of Sciences of the United States of America*, 76(1):91–5, January 1979.

- [35] Congyi Li, Andrew J Boileau, Ching Kung, and Julius Adler. Osmotaxis in *Escherichia coli*. *Proceedings of the National Academy of Sciences of the United States of America*, 85(24):9451–5, December 1988.
- [36] Richard P Blakemore, Richard B Frankel, and A J Kalmijn. South-seeking magnetotactic bacteria in the Southern Hemisphere. *Nature*, 286:384–5, 1980.
- [37] Richard B Frankel, Dennis A Bazylinski, Mark S Johnson, and Barry L Taylor. Magneto-aerotaxis in marine coccoid bacteria. *Biophysical Journal*, 73(2):994–1000, August 1997.
- [38] Julius Adler. Chemoreceptors in Bacteria. *Science*, 166(3913):1588–97, 1969.
- [39] Marco Montrone, Michael Eisenbach, Dieter Oesterhelt, and Wolfgang Marwan. Regulation of switching frequency and bias of the bacterial flagellar motor by CheY and fumarate. *Journal of Bacteriology*, 180(13):3375–80, July 1998.
- [40] Krishna Prasad, S Roy Caplan, and Michael Eisenbach. Fumarate modulates bacterial flagellar rotation by lowering the free energy difference between the clockwise and counterclockwise states of the motor. *Journal of Molecular Biology*, 280(5):821–8, July 1998.
- [41] Gladys Alexandre, Suzanne E Greer, and Igor B Zhulin. Energy taxis is the dominant behavior in *Azospirillum brasilense*. *Journal of Bacteriology*, 182(21):6042–8, November 2000.
- [42] Igor B Zhulin, Vyacheslav A Beshpalov, Mark S Johnson, and Barry L Taylor. Oxygen taxis and proton motive force in *Azospirillum brasilense*. *Journal of Bacteriology*, 178(17):5199–204, 1996.
- [43] Alexei Brooun, James Bell, Tracey Freitas, Randy W Larsen, and Maqsudul Alam. An archaeal aerotaxis transducer combines subunit I core structures of eukaryotic cytochrome c oxidase and eubacterial methyl-accepting chemotaxis proteins. *Journal of Bacteriology*, 180(7):1642–6, 1998.
- [44] Junichi Shioi, Rajanikant C Tribhuvan, Susan T Berg, and Barry L Taylor. Signal transduction in chemotaxis to oxygen in *Escherichia coli* and *Salmonella typhimurium*. *Journal of Bacteriology*, 170(12):5507–11, 1988.
- [45] Anuradha Rebbapragada, Mark S Johnson, Gordon P Harding, Anthony J Zuccarelli, Hansel M Fletcher, Igor B Zhulin, and Barry L Taylor. The Aer protein and the serine

- chemoreceptor Tsr independently sense intracellular energy levels and transduce oxygen, redox, and energy signals for *Escherichia coli* behavior. *Proceedings of the National Academy of Sciences of the United States of America*, 94(20):10541–6, 1997.
- [46] David E Gauden and Judith P Armitage. Electron transport-dependent taxis in *Rhodobacter sphaeroides*. *Journal of Bacteriology*, 177(20):5853–9, October 1995.
- [47] Jessica C Edwards, Mark S Johnson, and Barry L Taylor. Differentiation between electron transport sensing and proton motive force sensing by the Aer and Tsr receptors for aerotaxis. *Molecular Microbiology*, 62(3):823–37, November 2006.
- [48] Jong-Soon Choi, Young-Ho Chung, Yoon-Jung Moon, Changhoon Kim, Masakatsu Watanabe, Pill-Soon Song, Cheol-O Joe, Lawrence Bogorad, and Young Mok Park. Photomovement of the gliding cyanobacterium *Synechocystis* sp. PCC 6803. *Photochemistry and Photobiology*, 70(1):95–102, July 1999.
- [49] Shizue Yoshihara, Fumiko Suzuki, Hironori Fujita, Xiao Xing Geng, and Masahiko Ikeuchi. Novel putative photoreceptor and regulatory genes required for the positive phototactic movement of the unicellular motile cyanobacterium *Synechocystis* sp. PCC 6803. *Plant and Cell Physiology*, 41(12):1299–304, December 2000.
- [50] Ruslan N Grishanin, David E Gauden, and Judith P Armitage. Photoresponses in *Rhodobacter sphaeroides*: role of photosynthetic electron transport. *Journal of Bacteriology*, 179(1):24–30, 1997.
- [51] Vyacheslav A Bespalov, Igor B Zhulin, and Barry L Taylor. Behavioral responses of *Escherichia coli* to changes in redox potential. *Proceedings of the National Academy of Sciences of the United States of America*, 93(19):10084–9, September 1996.
- [52] Howard C Berg and Douglas A Brown. Chemotaxis in *Escherichia coli* analysed by Three-dimensional Tracking. *Nature*, 239:500–504, 1972.
- [53] Robert M Macnab and Daniel E Koshland Jr. The Gradient-Sensing Mechanism in Bacterial Chemotaxis. *Proceedings of the National Academy of Sciences of the United States of America*, 69(9):2509–2512, 1972.
- [54] Jeffrey E Segall, Steven M Block, and Howard C Berg. Temporal comparisons in bacterial chemotaxis. *Proceedings of the National Academy of Sciences of the United States of America*, 83(23):8987–91, December 1986.

- [55] Howard C Berg and P M Tedesco. Transient response to chemotactic stimuli in *Escherichia coli*. *Proceedings of the National Academy of Sciences of the United States of America*, 72(8):3235–9, August 1975.
- [56] Robert M Macnab. Bacterial flagella rotating in bundles: A study in helical geometry. *Proceedings of the National Academy of Sciences of the United States of America*, 74(1):221–5, January 1977.
- [57] Katherine A Borkovich, Nachum Kaplan, J Fred Hess, and Melvin I Simon. Transmembrane signal transduction in bacterial chemotaxis involves ligand-dependent activation of phosphate group transfer. *Proceedings of the National Academy of Sciences of the United States of America*, 86(4):1208–12, February 1989.
- [58] Martin Welch, Kenji Oosawa, Shin-Ichi Aizawa, and Michael Eisenbach. Phosphorylation-dependent binding of a signal molecule to the flagellar switch of bacteria. *Proceedings of the National Academy of Sciences of the United States of America*, 90(19):8787–91, October 1993.
- [59] J Fred Hess, Kenji Oosawa, Nachum Kaplan, and Melvin I Simon. Phosphorylation of Three Proteins in the Signaling Pathway of Bacterial Chemotaxis. *Cell*, 53(1):79–87, April 1988.
- [60] Wayne R Springer and Daniel E Koshland Jr. Identification of a protein methyltransferase as the cheR gene product in the bacterial sensing system. *Proceedings of the National Academy of Sciences of the United States of America*, 74(2):533–7, February 1977.
- [61] Jeffry B Stock and Daniel E Koshland Jr. A protein methylesterase involved in bacterial sensing. *Proceedings of the National Academy of Sciences of the United States of America*, 75(8):3659–63, August 1978.
- [62] Katherine A Borkovich, Lisa A Alex, and Melvin I Simon. Attenuation of sensory receptor signaling by covalent modification. *Proceedings of the National Academy of Sciences of the United States of America*, 89(15):6756–60, August 1992.
- [63] Hanbin Mao, Paul S Cremer, and Michael D Manson. A sensitive, versatile microfluidic assay for bacterial chemotaxis. *Proceedings of the National Academy of Sciences of the United States of America*, 100(9):5449–54, April 2003.

- [64] Mikhail N Levit and Jeffry B Stock. Receptor methylation controls the magnitude of stimulus-response coupling in bacterial chemotaxis. *The Journal of Biological Chemistry*, 277(39):36760–5, September 2002.
- [65] Victor Sourjik. Receptor clustering and signal processing in E. coli chemotaxis. *Trends in Microbiology*, 12(12):569–76, December 2004.
- [66] Robert Mesibov, George W Ordal, and Julius Adler. The range of attractant concentrations for bacterial chemotaxis and the threshold and size of response over this range. Weber law and related phenomena. *The Journal of General Physiology*, 62(2):203–23, August 1973.
- [67] Steven M Block, Jeffrey E Segall, and Howard C Berg. Adaptation kinetics in bacterial chemotaxis. *Journal of Bacteriology*, 154(1):312–23, April 1983.
- [68] Yevgeniy V Kalinin, Lili Jiang, Yuhai Tu, and Mingming Wu. Logarithmic sensing in Escherichia coli bacterial chemotaxis. *Biophysical Journal*, 96(6):2439–48, March 2009.
- [69] Oren Shoval, Lea Goentoro, Yuval Hart, Avi Mayo, Eduardo Sontag, and Uri Alon. Fold-change detection and scalar symmetry of sensory input fields. *Proceedings of the National Academy of Sciences of the United States of America*, 107(36):15995–6000, September 2010.
- [70] John L Spudich and Daniel E Koshland Jr. Non-genetic individuality: chance in the single cell. *Nature*, 262:467–71, 1976.
- [71] Naama Barkai and Stanislas Leibler. Robustness in simple biochemical networks. *Nature*, 387:913–917, 1997.
- [72] Uri Alon, Michael G Surette, Naama Barkai, and Stanislas Leibler. Robustness in bacterial chemotaxis. *Nature*, 397(January):168–171, 1999.
- [73] Markus Kollmann, Linda Lovdok, Kilian Bartholome, Jens Timmer, and Victor Sourjik. Design principles of a bacterial signalling network. *Nature*, 438(7067):504–7, November 2005.
- [74] Linda Lovdok, Kajetan Bentele, Nikita Vladimirov, Anette Muller, Ferencz S Pop, Dirk Lebiedz, Markus Kollmann, and Victor Sourjik. Role of Translational Coupling in Robustness of Bacterial Chemotaxis Pathway. *PLoS Biology*, 7(8):e1000171, August 2009.

- [75] Tau-Mu Yi, Yun Huang, Melvin I Simon, and John Doyle. Robust perfect adaptation in bacterial chemotaxis through integral feedback control. *Proceedings of the National Academy of Sciences of the United States of America*, 97(9):4649–53, April 2000.
- [76] Steven M Block, Jeffrey E Segall, and Howard C Berg. Impulse Responses in Bacterial Chemotaxis. *Cell*, 31(November):215–26, 1982.
- [77] Daniel E Koshland Jr. Biochemistry of sensing and adaptation in a simple bacterial system. *Annual Review of Biochemistry*, 50:765–82, January 1981.
- [78] Burton W Andrews, Tau-Mu Yi, and Pablo A Iglesias. Optimal Noise Filtering in the Chemotactic Response of *Escherichia coli*. *PLoS Computational Biology*, 2(11):e154, November 2006.
- [79] Nikita Vladimirov, Linda Lovdok, Dirk Lebiedz, and Victor Sourjik. Dependence of bacterial chemotaxis on gradient shape and adaptation rate. *PLoS Computational Biology*, 4(12):e1000242, December 2008.
- [80] Yigal Meir, Vladimir Jakovljevic, Olga Oleksiuk, Victor Sourjik, and Ned S Wingreen. Precision and kinetics of adaptation in bacterial chemotaxis. *Biophysical Journal*, 99(9):2766–74, November 2010.
- [81] Ekaterina Korobkova, Thierry Emonet, Jose M G Vilar, Thomas Simon Shimizu, and Philippe Cluzel. From molecular noise to behavioural variability in a single bacterium. *Nature*, 428:574–8, March 2004.
- [82] Thierry Emonet and Philippe Cluzel. Relationship between cellular response and behavioral variability in bacterial chemotaxis. *Proceedings of the National Academy of Sciences of the United States of America*, 105(9):3304–9, March 2008.
- [83] Hendrik Szurmant and George W Ordal. Diversity in Chemotaxis Mechanisms among the Bacteria and Archaea. *Microbiology and Molecular Biology Reviews*, 68(2):301–19, 2004.
- [84] Christopher V Rao, John R Kirby, and Adam P Arkin. Design and diversity in bacterial chemotaxis: a comparative study in *Escherichia coli* and *Bacillus subtilis*. *PLoS Biology*, 2(2):e49, February 2004.

- [85] Judith P Armitage and Robert M Macnab. Unidirectional, intermittent rotation of the flagellum of *Rhodobacter sphaeroides*. *Journal of Bacteriology*, 169(2):514–8, February 1987.
- [86] Ursula Attmannspacher, Birgit Scharf, and Rudiger Schmitt. Control of speed modulation (chemokinesis) in the unidirectional rotary motor of *Sinorhizobium meliloti*. *Molecular Microbiology*, 56(3):708–18, 2005.
- [87] David R Zusman, Ansley E Scott, Zhaomin Yang, and John R Kirby. Chemosensory pathways, motility and development in *Myxococcus xanthus*. *Nature Reviews Microbiology*, 5(11):862–72, November 2007.
- [88] Philip S Poole and Judith P Armitage. Motility response of *Rhodobacter sphaeroides* to chemotactic stimulation. *Journal of Bacteriology*, 170(12):5673–9, December 1988.
- [89] Sergei I Bibikov, Andrew C Miller, Khoosheh K Gosink, and John S Parkinson. Methylation-independent aerotaxis mediated by the *Escherichia coli* Aer protein. *Journal of Bacteriology*, 186(12):3730–7, 2004.
- [90] Bonnie B Stephens, Star N Loar, and Gladys Alexandre. Role of CheB and CheR in the complex chemotactic and aerotactic pathway of *Azospirillum brasilense*. *Journal of Bacteriology*, 188(13):4759–68, 2006.
- [91] Chuan V Dang, Mitsuru Niwano, Jun-Ichi Ryu, and Barry L Taylor. Inversion of Aerotactic Response in *Escherichia coli* Deficient in cheB Protein Methyltransferase. *Journal of Bacteriology*, 166(1):275–80, 1986.
- [92] Wouter D Hoff, Kwang-Hwan Jung, and John L Spudich. Molecular mechanism of photosignaling by archaeal sensory rhodopsins. *Annual Review of Biophysics and Biomolecular Structure*, 26:223–58, January 1997.
- [93] Shahid Khan, Robert M Macnab, Anthony L DeFranco, and Daniel E Koshland Jr. Inversion of a behavioral response in bacterial chemotaxis: explanation at the molecular level. *Proceedings of the National Academy of Sciences of the United States of America*, 75(9):4150–4, September 1978.
- [94] Steven L Porter, Anna V Warren, Angela C Martin, and Judith P Armitage. The third chemotaxis locus of *Rhodobacter sphaeroides* is essential for chemotaxis. *Molecular Microbiology*, 46(4):1081–94, November 2002.

- [95] Deepan S H Shah, Steven L Porter, Angela C Martin, Paul A Hamblin, and Judith P Armitage. Fine tuning bacterial chemotaxis: analysis of *Rhodobacter sphaeroides* behaviour under aerobic and anaerobic conditions by mutation of the major chemotaxis operons and *cheY* genes. *The EMBO Journal*, 19(17):4601–13, September 2000.
- [96] Kristin Wuichet and Igor B Zhulin. Origins and diversification of a complex signal transduction system in prokaryotes. *Science Signaling*, 3(128):ra50, January 2010.
- [97] Rebecca Hamer, Pao-Yang Chen, Judith P Armitage, Gesine Reinert, and Charlotte M Deane. Deciphering chemotaxis pathways using cross species comparisons. *BMC Systems Biology*, 4:3, January 2010.
- [98] George H Wadhams, A V Warren, Angela C Martin, and Judith P Armitage. Targeting of two signal transduction pathways to different regions of the bacterial cell. *Molecular Microbiology*, 50(3):763–70, August 2003.
- [99] Aldis Darzins. Characterization of a *Pseudomonas aeruginosa* gene cluster involved in pilus biosynthesis and twitching motility: sequence similarity to the chemotaxis proteins of enterics and the gliding bacterium *Myxococcus xanthus*. *Molecular Microbiology*, 11(1):137–53, January 1994.
- [100] Jesus Lacal, Cristina Garcia-Fontana, Francisco Munoz-Martinez, Juan-Luis Ramos, and Tino Krell. Sensing of environmental signals: classification of chemoreceptors according to the size of their ligand binding regions. *Environmental Microbiology*, 12(11):2873–84, November 2010.
- [101] Ariane Briegel, Davi R Ortega, Elitza I Tocheva, Kristin Wuichet, Zhuo Li, Songye Chen, Axel Muller, Cristina V Iancu, Gavin E Murphy, Megan J Dobro, Igor B Zhulin, and Grant J Jensen. Universal architecture of bacterial chemoreceptor arrays. *Proceedings of the National Academy of Sciences of the United States of America*, 106(40):17181–6, October 2009.
- [102] Mila Kojadinovic, Judith P Armitage, Marcus J Tindall, and George H Wadhams. Response kinetics in the complex chemotaxis signalling pathway of *Rhodobacter sphaeroides*. *Interface*, 10(81):20121001, 2013.
- [103] David M Harrison, Jennifer Skidmore, Judith P Armitage, and Janine R Maddock. Localization and environmental regulation of MCP-like proteins in *Rhodobacter sphaeroides*. *Molecular Microbiology*, 31(3):885–92, February 1999.

- [104] Ariane Briegel, Mark S Ladinsky, Catherine Oikonomou, Christopher W Jones, Michael J Harris, Daniel J Fowler, Yi-Wei Chang, Lynmarie K Thompson, Judith P Armitage, and Grant J Jensen. Structure of bacterial cytoplasmic chemoreceptor arrays and implications for chemotactic signaling. *eLife*, 3:e02151, January 2014.
- [105] Renyi Liu and Howard Ochman. Stepwise formation of the bacterial flagellar system. *Proceedings of the National Academy of Sciences of the United States of America*, 104(17):7116–21, April 2007.
- [106] Mark J Pallen and Nicholas J Matzke. From The Origin of Species to the origin of bacterial flagella. *Nature Reviews Microbiology*, 4(10):784–90, October 2006.
- [107] David M Faguy and Ken F Jarrell. A twisted tale: the origin and evolution of motility and chemotaxis in prokaryotes. *Microbiology*, 145(2):279–81, 1999.
- [108] Roger P Alexander and Igor B Zhulin. Evolutionary genomics reveals conserved structural determinants of signaling and adaptation in microbial chemoreceptors. *Proceedings of the National Academy of Sciences of the United States of America*, 104(8):2885–90, February 2007.
- [109] Travis J Muff and George W Ordal. The diverse CheC-type phosphatases: chemotaxis and beyond. *Molecular Microbiology*, 70(5):1054–61, December 2008.
- [110] Orkun S Soyer, Thomas Pfeiffer, and Sebastian Bonhoeffer. Simulating the evolution of signal transduction pathways. *Journal of Theoretical Biology*, 241(2):223–32, July 2006.
- [111] Paul Francois and Eric D Siggia. A case study of evolutionary computation of biochemical adaptation. *Physical Biology*, 5(2):026009, January 2008.
- [112] Richard A Goldstein and Orkun S Soyer. Evolution of taxis responses in virtual bacteria: non-adaptive dynamics. *PLoS Computational Biology*, 4(5):e1000084, May 2008.
- [113] Orkun S Soyer and Richard A Goldstein. Evolution of response dynamics underlying bacterial chemotaxis. *BMC Evolutionary Biology*, 11:240, 2011.
- [114] Matthew D Egbert, Xabier E Barandiaran, and Ezequiel A Di Paolo. A minimal model of metabolism-based chemotaxis. *PLoS Computational Biology*, 6(12):e1001004, January 2010.

- [115] Nicholas Blackburn, Tom Fenchel, and Jim Mitchell. Microscale Nutrient Patches in Planktonic Habitats Shown by Chemotactic Bacteria. *Science*, 282(5397):2254–2256, December 1998.
- [116] Roman Stocker, Justin R Seymour, Azadeh Samadani, Dana E Hunt, and Martin F Polz. Rapid chemotactic response enables marine bacteria to exploit ephemeral microscale nutrient patches. *Proceedings of the National Academy of Sciences of the United States of America*, 105(11):4209–14, March 2008.
- [117] Jens Efsen Johansen, Jarone Pinhassi, Nicholas Blackburn, Ulla Li Zweifel, and Ake Hagstrom. Variability in motility characteristics among marine bacteria. *Aquatic Microbial Ecology*, 28:229–237, 2002.
- [118] Tanvir Ahmed, Thomas Simon Shimizu, and Roman Stocker. Microfluidics for bacterial chemotaxis. *Integrative Biology*, 2(11-12):604–29, November 2010.
- [119] Nicholas Blackburn and Tom Fenchel. Influence of bacteria, diffusion and shear on micro-scale nutrient patches, and implications for bacterial chemotaxis. *Marine Ecology Progress Series*, 189:1–7, 1999.
- [120] Antonio Celani and Massimo Vergassola. Bacterial strategies for chemotaxis response. *Proceedings of the National Academy of Sciences of the United States of America*, 107(4):1391–6, January 2010.
- [121] Damon A Clark and Lars C Grant. The bacterial chemotactic response reflects a compromise between transient and steady-state behavior. *Proceedings of the National Academy of Sciences of the United States of America*, 102(26):9150–5, June 2005.
- [122] United States The MathWorks, Inc., Natick, Massachusetts. MATLAB and Image Processing Toolbox Release 2013a, 2013.
- [123] Victor Sourjik and Howard C Berg. Receptor sensitivity in bacterial chemotaxis. *Proceedings of the National Academy of Sciences of the United States of America*, 99(1):123–7, January 2002.
- [124] James G Mitchell. The energetics and scaling of search strategies in bacteria. *The American Naturalist*, 160(6):727–40, December 2002.
- [125] Edward M Purcell. Life at low Reynolds number. *American Journal of Physics*, 45(1):3–11, 1977.

- [126] James G Mitchell. The influence of cell size on marine bacterial motility and energetics. *Microbial Ecology*, 22(1):227–38, 1991.
- [127] Mark J Schnitzer. Theory of continuum random walks and application to chemotaxis. *Physical Review E*, 48(4):2553–68, 1993.
- [128] P-G de Gennes. Chemotaxis: the role of internal delays. *European Biophysics Journal*, 33(8):691–3, December 2004.
- [129] Rudolf Gotz and Rudiger Schmitt. Rhizobium meliloti swims by unidirectional, intermittent rotation of right-handed flagellar helices. *Journal of Bacteriology*, 169(7):3146–50, July 1987.
- [130] Yariv Kafri and Rava Azeredo da Silveira. Steady-state chemotaxis in Escherichia coli. *Physical Review Letters*, 100(23):1–4, 2008.
- [131] Philippe Cluzel, Michael G Surette, and Stanislas Leibler. An Ultrasensitive Bacterial Motor Revealed by Monitoring Signaling Proteins in Single Cells. *Science*, 287(5458):1652–1655, March 2000.
- [132] Dennis Bray, Matthew D Levin, and Carl J Morton-Firth. Receptor clustering as a cellular mechanism to control sensitivity. *Nature*, 393:85–88, 1998.
- [133] T A J Duke and Dennis Bray. Heightened sensitivity of a lattice of membrane receptors. *Proceedings of the National Academy of Sciences of the United States of America*, 96(18):10104–8, August 1999.
- [134] Jason E Gestwicki and Laura L Kiessling. Inter-receptor communication through arrays of bacterial chemoreceptors. *Nature*, 415(6867):81–4, January 2002.
- [135] Naama Barkai, Uri Alon, and Stanislas Leibler. Robust amplification in adaptive signal transduction networks. *Comptes Rendus de l'Academie des Sciences - Serie IV - Physique et Astrophysique*, 2(6):871–7, 2001.
- [136] Siebe B van Albada and Pieter Rein ten Wolde. Differential affinity and catalytic activity of CheZ in E. coli chemotaxis. *PLoS Computational Biology*, 5(5):e1000378, May 2009.
- [137] Orkun S Soyer, Hiroyuki Kuwahara, and Attila Csikasz-Nagy. Regulating the total level of a signaling protein can vary its dynamics in a range from switch like ultrasensitivity to adaptive responses. *The FEBS Journal*, 276(12):3290–8, June 2009.

- [138] Colin J Ingham and Judith P Armitage. Involvement of transport in *Rhodobacter sphaeroides* chemotaxis. *Journal of Bacteriology*, 169(12):5801–7, December 1987.
- [139] Yehudit Jeziore-Sassoon, Paul A Hamblin, Carolyn A Bootle-Wilbraham, Philip S Poole, and Judith P Armitage. Metabolism is required for chemotaxis to sugars in *Rhodobacter sphaeroides*. *Microbiology*, 144(1):229–39, January 1998.
- [140] Angela C Martin, Marcus Gould, Elaine Byles, Mark A J Roberts, and Judith P Armitage. Two chemosensory operons of *Rhodobacter sphaeroides* are regulated independently by sigma 28 and sigma 54. *Journal of Bacteriology*, 188(22):7932–40, November 2006.
- [141] Rina Barak, Jianshe Yan, Alla Shainskaya, and Michael Eisenbach. The chemotaxis response regulator CheY can catalyze its own acetylation. *Journal of Molecular Biology*, 359(2):251–65, June 2006.
- [142] Gabriel Zarbiv, Hui Li, Amnon Wolf, Gary Cecchini, S Roy Caplan, Victor Sourjik, and Michael Eisenbach. Energy complexes are apparently associated with the switch-motor complex of bacterial flagella. *Journal of Molecular Biology*, 416(2):192–207, February 2012.